Trading in cooperativity for specificity to maintain uracil-free DNA

Judit E. Szabó[1], Enikő Takács[1], Gábor Merényi[1#], Beáta G. Vértessy[1,2], Judit Tóth[1]

[1]Institute of Enzymology, Research Centre for Natural sciences, Hungarian Academy of sciences, Budapest, Hungary

[2]Department of Applied Biotechnology and Food Science, Budapest University of Technology and Economics, Budapest, Hungary

[#]present address: Department of Molecular Biosciences, The Wenner-Gren Institute, Stockholm University

Abstract

Members of the dUTPase superfamily play an important role in the maintenance of the pyrimidine nucleotide balance and of genome integrity. dCTP deaminases and the bifunctional dCTP deaminase-dUTPases are cooperatively regulated by dTTP. However, the manifestation of allosteric behavior within the same trimeric protein architecture of dUTPases, the third member of the superfamily, has been a question of debate for decades. Therefore, we designed hybrid dUTPase trimers to access conformational states potentially mimicking the ones observed in the cooperative relatives. We studied how the interruption of different steps of the enzyme cycle affects the conformational distribution of non-mutated active sites. The results combined with a comparative structural analysis of dUTPase superfamily enzymes reveal an intriguing trade-off between regulation and efficiency. We demonstrate that the lack of allosteric regulation in dUTPase is related to the functional adaptation to uracil-DNA prevention.

Allosteric characteristics of protein-ligand interactions present a research field with great traditions but also with key current interest [1,2]. Recent developments in the understanding of the manifestation of allosteric behavior within a given protein architecture lead to a shift from the classical view to a more subtle dynamic view. According to the classical view, allostery is based on a series of distinct structural changes leading to functionally different conformers of a given protein. However, several examples demonstrated that the allosteric behavior does not necessarily require switches between direct conformers [3] but can be explained by alterations of side chain [4] or main chain dynamics [5] or by a shift in the distribution of preexisting protein conformations [6]. In the present study, we set out to investigate the manifestation of allostery within the superfamily of dUTPases. The superfamily comprises the dUTPase, dCTP deaminase (DCD) and the bifunctional dCTP deaminase-dUTPase (DCD-DUT) enzymes that produce dUMP, the obligatory *de novo* dTTP synthesis precursor from either dUTP or dCTP, respectively (Fig 1). The removal of dUTP from the cellular dNTP pool is also a vital function of dUTPases. These enzymes thus play an important role in the maintenance of the pyrimidine nucleotide balance and genome integrity [7–13]. dUTPase and DCD(-DUT) share a common homotrimeric structural core [14–17] (Fig 2A). The three subunits form a central channel and three equivalent active sites at the intersubunit clefts (Fig 2A). This intricate quaternary structure intuitively suggests the possibility for allosteric control within the enzyme. In effect, the allosteric communication between the active sites of DCD family enzymes has been investigated in several species[16,18–20] and was found to operate through the central channel[16,20]. The cooperative conformational change in these enzymes occurs in a loop (referred to as allosteric loop from now on) located at the interface of the nucleotide binding site and the central channel (Fig 2B). The allosteric loop can adopt the mutually exclusive active and inactive conformations. The conformational change of one loop facilitates the same conformational change in the other two loops of the trimer due to steric hindrance within the central channel [16,20]. This mechanism thus conforms to the classical view of allostery.

dUTPases, the other family that belongs to the dUTPase superfamily, display an even more intricate interaction pattern between their subunits than DCDs do. The C-terminal arm of dUTPases in almost all cases reaches across the trimer to the remote active site and therefore, all three subunits provide conserved residues to each active site [17]. This structure inspired the proposition that allosteric communication between the active sites of dUTPases should also exist [21–23]. Crystallographic observations in the human dUTPase suggested that some allosteric effect must help the release of the dUMP product [21]. Another study investigating the nature of the central channel of dUTPases found considerable difference in hydropathy between eukaryotic and prokaryotic dUTPases [22]. It was proposed that allostery can emerge through the hydrophilic central channel in eukaryotic dUTPases. A later NMR study suggested that the *Drosophila* enzyme exhibits cooperativity in both substrate and product binding based on signal intensity titrations well above the K_d of the respective complexes [23]. In the EIAV (Equine Infections Anemia Virus) enzyme, a Trp at the central channel senses the nucleotide-bound states of the active site [24] corroborating the potential of active site communication through the central channel. On the other hand, detailed kinetic analyses of dUTPases from various species (human [25], *E. coli* [26], EIAV [24], *Plasmodium falciparum* [27]) failed to directly detect any cooperative behavior in the enzymatic mechanism.

The cooperativity in DCD is best observed when dTTP, its feedback inhibitor binds to the active site. As the accommodation of the additional metal group on the thymine ring is possible only in the inactive conformation [16,20], the shift in the equilibrium between the active and inactive conformational states and the cooperative behavior is more pronounced in the presence of dTTP [16,20,28]. The substrate binding pocket of dUTPases, however, does not accommodate other bases than uracil with considerable affinity [21,26,29]. This property of dUTPases may make it difficult to recognize any allosteric behavior potentially manifested as alterations of conformational distribution. The inherent allosteric potential in proteins may only appear by mutations that shift the distribution of the various conformational states [6,30]. Therefore, we designed mutations to access inactive conformational states in dUTPase potentially mimicking the ones observed in DCD and DCD-DUT. To this end, we created covalently linked human dUTPase pseudoheterotrimers (called hybrids henceforth) in which the active sites could be turned off selectively (Fig 2C). We studied how the interruption of different steps of the enzyme cycle in one active site of the hybrid affects the conformational distribution of the non-mutated active sites using various enzymatic and structural biology approaches. Our experimental results combined with the comparative analysis of the structural features of dUTPase superfamily enzymes reveals an intriguing trade-off between regulation and efficiency, two ways of functional adaptation to distinct metabolic functions.

Results

Establishment and enzyme activity of asymmetric dUTPase hybrids

Mutations introduced to a homooligomeric protein appear in each subunit as the oligomer is assembled from identical monomers (Fig 3A). To generate hybrid enzymes of the human dUTPase (hDUT), we therefore needed to create a covalently linked pseudohomotrimer (termed WWW) in which each subunit could be exchanged to selectively contain the desired mutation (Fig 3B). The WWW construct was assembled from the previously described sensor-bearing $hDUT^{F158W}$ human dUTPase [25,31] monomers (W) connected with well-described flexible peptide linkers [32] (see Online Methods and Supplementary Table 1). The F158W substitution enables the fluorescent monitoring of certain enzymatic reaction steps without altering the mechanism [25,33,34]. We introduced each further mutation into this WWW scaffold by exchanging one or more of the W cassettes.

To test whether the linkers influence the enzymatic properties of the WWW enzyme, we applied transient kinetic analysis using the fluorescent signal of W158. The kinetic parameters of substrate binding and hydrolysis as well as the characteristic fluorescence changes during the course of the reaction remained similar in WWW to that measured in $hDUT^{F158W}$ (Supplementary Fig 1, Table 1). We also performed limited tryptic digestion of the covalent enzyme to cleave the linkages between the subunits. The cleaved enzyme displayed basically identical steady-state and transient kinetic properties to that of the covalently linked one (Supplementary Fig 2). We concluded that the linkers do not influence the enzymatic mechanism and thus the covalent enzyme is suitable for further investigations.

Four different hybrid enzymes were subsequently created to investigate the possible allosteric effects of conformational changes upon substrate binding, hydrolysis or product release (Fig 4A).

To investigate the allosteric effect of a possible global conformational change upon substrate binding, we created an active site that is unable to accommodate the uracil ring (Supplementary Fig 3A) and is thus defective in substrate binding and any conformational change coupled to it. Control experiments with the homotrimeric form of the A98F mutant ($hDUT^{F158W,\ A98F}$) confirmed that it could not bind the substrate and was entirely inactive (Supplementary Fig 3B-F). We introduced this mutation to the covalent construct to obtain WWF.

The following constructs were designed to investigate whether conformational changes occurring upon hydrolysis or product release are necessary to be transmitted to neighboring active sites for the global activity of the trimer.

In the WWN and WNN constructs, the conserved catalytic Asp from the third conserved motif was changed to Asn (Supplementary Fig 3G) in one or two active sites, respectively. This Asp/Asn substitution has been described to reduce the catalytic activity close to zero while the substrate binding properties do not change [10,35]. We also tested the enzymatic properties of $hDUT^{D102N,\ F158W}$ and found that the catalytic activity decreased below the detectable level (< 0.002 s^{-1}) both under steady-state and single turnover conditions while the substrate binding properties remained unaffected compared to $hDUT^{F158W}$ (Supplementary Fig 3H).

In the WWS enzyme, we removed the C-terminal P-loop-like motif of the last subunit of the pseudoheterotrimer. This conserved motif interacts with the γ-phosphate of dUTP and stacks over the uracil ring to orient the catalytic apparatus and stabilize the transition state [31,33,34,36]. The P-loop-like motif is only present in dUTPases and is missing from DCDs or DCD-DUTs. Its removal results in major decrease (~ 720 fold) of the catalytic constant and minor (~ 3 fold) increase in the dissociation constant of the enzyme-substrate complex [31].

dUTPase active sites work independently from each other

Potential allosteric interactions within the hybrids WWN, WNN, WWS and WWF were analyzed using the combination of steady state and transient kinetic measurements. All constructs proved to be active indicating that the arrest of the enzyme cycle in a given active site does not compromise the enzymatic turnover in the others. Steady-state activity titrations of all hybrid enzymes exhibited Michaelis-Menten kinetics (Fig 4B). The maximal initial velocities (V_{max}) decreased proportionally with the number of inactivated sites, i.e. WWN, WWF and WWS displayed about 2/3, while WNN displayed approximately 1/3 activity compared to WWW (Fig 4C, Table I.). This indicates that the activity per working subunit is

unaltered in the hybrid enzymes. The Michaelis constants did not change considerably compared to the WT (Table 1). Single turnover stopped-flow measurements showed that the kinetic mechanism of the asymmetric hybrids is identical with that of the control WWW (Supplementary Fig 4). The k_{obs} for substrate binding and the single turnover rate constants (k_{STO}) remained unaltered (Table 1, Fig 4C). This implies that the observed decrease in the steady-state activity is only due to the decreased active site concentration.

The kinetics of substrate binding to the hybrid enzymes was also investigated under pseudo first order conditions. A large part of the time courses got lost in the dead-time of the instrument which hindered the determination of the rate constants. The total signal change, however, could be used to determine the dissociation constants (K_d) of the enzyme-dUTP complexes (Fig 4D). The obtained K_d-s were similar to that of the WWW-dUTP complex (Table 1).

In summary, a global active to inactive conformational transition observable in DCDs could not be identified in dUTPase even in conditions potentially mimicking the asymmetry in a partially dTTP-saturated DCD enzyme (Fig 2C). On the contrary, Fig 4C clearly indicates that the active sites turn over independently from each other. In case of a cooperative transition to a global inactive state we would expect inactivity following the first turnover or non-proportional activity decrease in the hybrid enzymes containing one or two defective active sites.

The conformational flexibility of human dUTPase is restricted by Mg^{2+} binding to the central channel

The conformational changes resulting in the observed cooperative behavior is transmitted through the central channel in DCD family enzymes. We therefore investigated the structural features of the channel possibly responsible for the lack of conformational transmission in dUTPase. The site of cooperative conformational change of DCD(-DUT) enzymes corresponds to one of the two suggested Mg^{2+} binding sites in the human dUTPase [21,37] (Asp95, Fig 5A). In contrast, no metal binding to DCD(-DUT) enzymes has been reported.

To evaluate the role of Mg^{2+} binding to the central channel of $hDUT^{F158W}$, we conducted in solution structural investigations in the presence and absence of Mg^{2+}. The near-UV CD spectra showed considerable changes upon the addition of Mg^{2+} to the apo $hDUT^{F158W}$ indicating that the metal ion binds to the enzyme and modifies its structure (Fig 5B). The largest signal change was observable at 285 nm probably yielded by the rearrangement of Tyr residues (Fig 5A). The far-UV CD spectra, on the other hand, showed only minor changes upon Mg^{2+} addition (Fig 5B inset) implying that metal binding may not induce major changes in the secondary structure. The WWW enzyme showed similar spectral changes to $hDUT^{F158W}$ upon the addition of Mg^{2+} (Supplementary Fig 5 A,B).

The thermal denaturation of $hDUT^{F158W}$ could be described with a two-state equilibrium model indicating that the heat-induced unfolding of the trimer happens in one step, without a significantly populated intermediate state of dissociated and folded monomers

[38] (Fig 5C). In the absence of Mg^{2+}, we observed a slight but reproducible decrease in the melting temperature (T_m) (Fig 5C) suggesting that the stability of the enzyme is slightly decreased in the absence of Mg^{2+} similarly to what was found in the *D. melanogaster* dUTPase [39]. The covalent WWW enzyme produced a more complicated melting curve (Supplementary Fig 5C). However, the stabilization effect of Mg^{2+}could also be observed.

To test the potentially increased flexibility of $hDUT^{F158W}$ in the absence of Mg^{2+}, we performed limited trypsinolysis. $hDUT^{F158W}$ was highly sensitive to tryptic digestion in the absence of Mg^{2+} (Fig 5D and Supplementary Fig 6) whereas the control *Mycobacterium tuberculosis* dUTPase (mtDUT) that does not contain Mg^{2+} binding sites in its central channel (Fig 6F) was not (Fig 5D and Supplementary Fig 6). Following the expected cleavage of the flexible N- and C-termini [33], the remaining enzyme core – which is otherwise stable for long time – disappeared within an hour (Fig 5D). In case of the mtDUT, the enzyme core remained stable during the one our experiment. This phenomenon indicates that the quaternary structure of $hDUT^{F158W}$ is significantly more flexible in the absence than in the presence of Mg^{2+}.

Structural comparison of dUTPase superfamily enzymes reveals trade-off in conformational flexibility and active site specificity

To understand the structural basis of the mechanistic differences within the dUTPase superfamily, we compared the central channel, the region of the allosteric loop and the nucleobase binding region in DCDs and dUTPases (Fig 6).

The amino acids responsible for the binding of the nucleobase are located around motif 3 (Fig 6A) at the N- and C-terminal parts of the β-hairpin accommodating the nucleoside (Fig 6B). The N-terminal few amino acids of the β-hairpin overlap with the allosteric loop in the DCD family. We found that this region is highly diverse in size and amino acid composition within the superfamily (Fig 6A-B).

In eukaryotic dUTPases, the loop is shorter by 2 or 3 amino acids than in DCDs resulting in a tighter uracil binding cleft. In these enzymes, mostly main chain atoms establish hydrogen bonding interactions with the nucleobase, which was proposed to contribute to their specificity for uracil [21]. The very same loop confers the Mg^{2+} binding site facing the central channel (Fig 6C, Fig 5A).

In retroviral dUTPases (EIAV shown as the representative), the loop is even shorter than that of the Mg^{2+} binding site-bearing eukaryotic dUTPases (Fig 6A-B).

The allosteric loop of prokaryotic dUTPases is of the same length as that of DCDs. However, its amino acid composition is different (Fig 6A) resulting in a tighter central channel mainly due to the LV/SM/SP/AP peptides protruding in it (Fig 6A-B). The conformational flexibility of the channel is restricted by the hydrophobic interactions of the modified allosteric loop (Fig 6D) or by a conserved Pro (Fig 6E). In DCDs, the conserved Ala of the allosteric loop engages in H-bonding with the oxo group of the substrate uracil. If thymine is bound to the active site, the HVTA peptide containing this Ala moves into the channel (cf. Fig 2B). In contrast, a conserved Asn plays the same H-bonding role in prokaryotic dUTPases but it resides in a conformationally restricted peptide (Fig 6A, D-E).

The sequence and structural comparison with DCD enzymes reveals that the various evolutionary branches of dUTPases possess an altered or shortened allosteric loop which

coincides with the conformational stabilization of the central channel. Interestingly, most of the observed alterations contribute to the specificity for dUTP at the same time. We propose that the central channel of dUTPases features increased stability at the cost of lacking the potential for mediating cooperativity as observed in DCDs. Apparently, the same structural element of the active site is responsible for substrate specificity and for the communication through the central channel.

Discussion

Allosteric enzyme regulation is one of the general means of controlling biochemical processes. The appropriate concentration and balance of dNTPs for DNA synthesis and repair is commonly regulated by both homotrop and heterotop allosteric mechanisms [40,41]. Feedback inhibition by dTTP in two of the three dUTPase superfamilies, DCDs and the bifunctional DCD-DUTs (Fig 1), seems to be important to maintain the appropriate dCTP/ dTTP ratio [10,16,20]. The feedback inhibitor dTTP binds to the active sites which communicate with each other within the homotrimer resulting in an all-or-none inhibition pattern. This is a more complicated and more efficient inhibition mechanism than simple competitive inhibition due to the fact that 1 dTTP molecule elicits the complete inhibition of 3 active sites. Interestingly, the activity of the non-homologous dCMP deaminases is also modified by dCTP and dTTP with intricate regulation pattern involving cooperativity [42–44]. Probably, this kind of regulation is important in maintaining the correct dCTP / dTTP ratio [45].

We attempted to detect allosteric behavior in dUTPases by engineering hybrid enzymes to restrict putative allosteric transmission between active sites at various stages of the enzymatic cycle. Interestingly, however, the enforced asymmetry in the dUTPase trimer did not elicit any instance of cooperative behavior despite the fact that dUTPases have the most intertwined trimeric structure of all within the dUTPase superfamily. We determined that i) the active sites work independently from each other; ii) Mg^{2+} binding in the central channel reduces the flexibility and increases the thermal stability of the quaternary structure; iii) the allosteric loop that connects the active site to the central channel is conformationally restricted in dUTPases compared to DCD family enzymes. This phenomenon is interrelated with structural solutions for increased dUTP specificity in every case.

It is common in enzyme evolution that mutations in flexible active site loops are responsible for altered substrate specificity [46]. Since active sites are often located at intersubunit / interdomain clefts, these flexible loops have a potential to mediate allosteric communication between the active sites. In our case, it seems that the specialization for a single substrate results in the loss of allosteric communication. The shorter / less flexible allosteric loop compared to that of DCDs and DCD-DUTs is related to increased dUTP specificity (Fig 6). Another “dUTPase invention” is the C-terminal P-loop-like motif that discriminates against dUDP and makes dUTP hydrolysis more efficient by several orders of magnitude than DCD-DUTs [31]. The gain of specificity together with the enhancement of the catalytic power represent features that make dUTPases significantly more powerful in dUTP breakdown as compared to DCD-DUTs. This advance may be necessary to avoid the appearance of the non-canonical uracil base in DNA [10] that induces the activation of DNA

repair mechanisms upon non-physiological uracil accumulation leading to severe to fatal consequences for the cell [47–49]. The cooperative allosteric behavior in DCDs and DCD-DUTs, on the other hand, make these enzymes suitable for the regulation of the nucleotide pool. We propose that the trade-off between cooperativity and specificity in the dUTPase superfamily represents instances of adaptation to the distinct roles of dUMP production for dTTP synthesis and dUTP elimination for uracil-DNA avoidance, respectively.

Online Methods

Reagents. Molecular biology products were from New England Biolabs (US) and Fermentas (Canada), electrophoresis and chromatography reagents were from Bio-Rad (US) and Qiagen (Netherland). Phenol red was from Merck (Germany). dUMP, dUDP and α,β-imido-dUTP (dUPNPP) was from Jena Bioscience (Germany), dUTP and other chemicals were from Sigma–Aldrich (US).

Cloning and mutagenesis. Site-directed mutagenesis was performed by the QuikChange method (Stratagene) and was verified by sequencing. The enzyme conferring a tryptophan sensor in the active site ($hDUT^{F158W}$) was used as wild-type [25,33,34]. The following mutants were created within this construct: Asp102 to Asn ($hDUT^{F158W,\ D102N}$) and Ala98 to Phe ($hDUT^{F158W,\ A98F}$). Mutagen forward and reverse primers are presented in Supplementary Table 1. The covalent wild type enzyme (WWW) was created by genetic engineering. $hDUT^{F158W}$ was amplified with primers encoding linkers and various restriction sites (Supplementary Table 1) to create the three subunits of WWW. The subunits were cloned to pET45b plasmid as individual restriction cassettes. Covalent pseudoheterotrimers (hybrids) were then created by changing one or two of the wild type cassettes in WWW to mutant one(s).

Protein expression and purification. Expression and purification of noncovalent human dUTPase proteins were done as described previously in Varga *et al*. 2007 FEBS Letters[33]. Covalent dUTPase pseudotrimers were expressed and purified similarly, except that BL21 Rosetta (pLysS) cells (Novagen) were used instead of BL21. The expression and purification of the His-tagged *Mycobacterium tuberculosis* dUTPase (mtDUT) was done based on Varga *et al*. 2008 BBRC[50]. The protein concentration was measured using the Bradford method (Bio-Rad Protein Assay) and by UV absorbance. Extinction coefficients were calculated based on the amino acid sequence using the ProtParam tool (http://web.expasy.org/protparam/). Extinction coefficients for the proteins were: λ_{280}=16055 $M^{-1}cm^{-1}$ for the $hDUT^{F158W}$, $hDUT^{F158W,D102N}$ and $hDUT^{F158W,\ A98F}$; λ_{280}=48290 $M^{-1}cm^{-1}$ for the WWW, WWF, WWN and WNN and λ_{280}=42790 $M^{-1}cm^{-1}$ for the WWS construct. Protein concentration is given in monomer/subunit concentration in every case. All measurements were carried out in a buffer comprising 20 mM HEPES pH 7.5, 100 mM NaCl, 2 mM $MgCl_2$ and 2 mM ß-mercaptoethanol ("assay buffer") if not stated otherwise.

Steady-state colorimetric dUTPase assay was performed as described in Varga *et al*. 2008 BBRC[50]. This phenol red indicator assay was used to detect the protons released in the dUTPase reaction. 0.01-1 μM protein was used for the dUTPase assay in a buffer containing 1 mM HEPES pH 7.5, 100 mM KCl, 40 μM phenol red and 5 mM $MgCl_2$. A Specord 200 spectrophotometer (Analytic Jena, Germany) and 10 mm path length thermostatted cuvettes were used at 20 ^oC and absorbance was recorded at 559 nm. The initial velocity was determined from the first 10 % of the progress curves. Initial velocities were plotted against substrate concentration and the results were fitted with the Michaelis–Menten equation.

Fluorescence measurements. Fluorescence spectra and intensity titrations were recorded on a Jobin Yvon Spex Fluoromax-3 spectrofluorometer in the assay buffer at 20 ^{o}C. Trp fluorescence was excited at 297 nm, emission spectra were recorded between 320-400 nm while the fluorescence intensity titrations were detected at 345 nm. Additional fluorescence or inner filter effect imposed on the measured intensities during the titration experiments were corrected by subtracting the corresponding buffer spectra. Titration data were fitted with the equation describing 1:1 stoichiometry for the dissociation equilibrium assuming no cooperativity:

$$y = s + \frac{A\left[(c + x + K) - \sqrt{(c + x + K)^2 - 4cx}\right]}{2c}$$

(Equation 1)

where x is the ligand concentration and y is the fluorescence intensity, $s = y$ at $x = 0$, A is the amplitude of the fluorescence intensity change, c is the enzyme concentration and K is the dissociation constant of the ligand complex.

Thermofluor assay. Thermal shift assays were carried out on an Mx3000P® QPCR System (Agilent Technologies Company). Thermal shift reactions were performed in a 96-well thin-wall microplate in a total volume of 25 µl containing 500 x diluted Sypro® Orange dye. Samples were heated from 25.0 to 80.0 ^{o}C. The speed of heating was 1 °C / minute. The protein concentration of hDUT^{F158W} was 0.8 mg / ml in the measurements, while the WWW enzyme was used at 2 mg / ml concentration. To compensate for the difference in the ionic strength between the samples with and without $MgCl_2$, NaCl was added according to Equation 2:

$$I = 0.5 * \sum (c_i * z_i^2)$$

(Equation 2)

where I is the ionic strength, c_i is the concentration, z_i is the charge of the particular ion and i is the index of summation.

The raw data of the heat-induced unfolding monitored by fluorescence emission were converted to the apparent fraction of native protein F_N, according to Equation (3):

$$F_N = \frac{(\theta_U + m_U * T) - \theta}{(\theta_U + m_U * T) - (\theta_N + m_N * T)}$$

(Equation 3)

where Θ is the observed spectroscopic signal at temperature T, Θ_N and Θ_U are the intercepts and m_N and m_U are the slopes of the pre- and post-transitional base lines of the raw data, respectively. The F_N vs. T plot was converted to the F_U vs. T plot by using the $F_N + F_U = 1$ equation, where F_U is the fraction of unfolded protein. The F_U vs. T plot was then fitted with the Boltzmann or the double Boltzmann equation (Equations 4 and 5) to determine the midpoint of the transition(s)

$$y = \frac{A_1 + A_2}{1 + e^{\frac{x - x_0}{dx}}} + A_2$$

(Equation 4)

where *A1* and *A2* are the pre- and post-transitional base lines and x_0 is the transition midpoint.

$$y = y_0 + A\left(\frac{p}{1 + e^{\frac{x - x_{01}}{k_1}}} + \frac{1 - p}{1 + e^{\frac{x - x_{02}}{k_2}}}\right)$$

(Equation 5)

where *A* is the total signal change, *p* is the fraction of the first transition, k_1 and k_2 are the slope factors of the two transitions, y_0 is the offset, while x_{01} and x_{02} are the transition midpoints.

Circular dichroism measurements. CD spectra recording was carried out in a JASCO 720 spectropolarimeter at 20 ^{o} C using a quartz cuvette with 1 mm (far UV) or 10 mm (near UV) path length. Far UV and near UV spectra were recorded at 200-250 nm or 250-300 nm, respectively. All protein containing spectra were corrected by subtracting the corresponding buffer spectra.

Fast kinetics experiments. Fluorescence stopped-flow measurements were carried out at 20 ^{o}C using an SX-20 stopped-flow apparatus (Applied Photophysics, UK) as described previously [25]. Equal volumes (50 µl) of dUTPase enzyme and dUTP solutions were mixed and 8 traces were recorded and averaged for each time course. Under single turnover conditions, a triple exponential equation was fitted to the averaged traces to determine the catalytic constants based on Tóth *et al.* 2007 JBC [25]. For the determination of binding rate constants, the ligand titration was performed under pseudo-first order conditions. The observed rate constants for the two binding steps described previously (collision complex formation and isomerisation)[25] were determined by fitting double exponential equations. Where exponential equation for the first part of the time course could not been fitted due to the large signal loss in the dead time, the K_d was estimated by plotting the amplitudes of the fluorescence decrease against ligand concentration followed by fitting a hyperbola.

Limited trypsinolysis. The limited tryptic digestion of dUTPases was performed at 37 ^{o} C using 0.5 mg / ml protein concentration and 1:20 trypsin : dUTPase ratio in assay buffer also containing either 0.1 mM EDTA or 5 mM $MgCl_2$. The tryptic digestion was terminated by the addition of 1 mM PMSF to the samples taken at different time points. The time dependence of the trypsinolysis was analyzed on SDS-PAGE. Limited trypsinolysis in the presence of 1 mM α,β-imido-dUTP was performed likewise in the same buffer either with or without Mg^{2+}. SDS-PAGE gels were analyzed by densitometry with the UVIdoc software.

The cleavage of the linkers of the WWN covalent enzymes was performed at 25 ^{o} C using 0.8 mg / ml protein concentration and 1:500 trypsin : dUTPase ratio in the assay buffer also containing 1 mM α,β-imido-dUTP for the protection of the C-terminus [33] and 5 mM $MgCl_2$. The digestion was terminated by the addition of 1 mM benzamidine hydrochloride after 5 minutes. The sample was dialyzed against assay buffer containing 1mM benzamidine and 5mM $MgCl_2$ to remove α,β-imido-dUTP. The control sample was treated similarly without the addition of trypsin. The trypsinolysis product, the W/W/N heterotrimer, was analysed on SDS-PAGE and by enzymatic assays.

Data fitting and statistical analysis. Data fitting was performed using Origin 7.5 (OriginLab Corp., Northampton, MA) or the stopped-flow software. Error bars represent the standard deviation of the mean of several measurements depending on the type of assay (detailed at each Method section and in the legends of the Figures and Tables).

References

1. Changeux, J.-P. Allostery and the Monod-Wyman-Changeux model after 50 years. *Annu. Rev. Biophys.* **41,** 103–33 (2012).

2. Changeux, J.-P. 50 Years of Allosteric Interactions: the Twists and Turns of the Models. *Nat. Rev. Mol. Cell Biol.* **14,** 819–29 (2013).

3. Motlagh, H. N., Wrabl, J. O., Li, J. & Hilser, V. J. The ensemble nature of allostery. *Nature* **508,** 331–9 (2014).

4. Petit, C. M., Zhang, J., Sapienza, P. J., Fuentes, E. J. & Lee, A. L. Hidden dynamic allostery in a PDZ domain COMPUTATIONAL BIOLOGY. 3–8 (2009).

5. Tzeng, S.-R. & Kalodimos, C. G. Dynamic activation of an allosteric regulatory protein. *Nature* **462,** 368–72 (2009).

6. Gunasekaran, K., Ma, B. & Nussinov, R. Is allostery an intrinsic property of all dynamic proteins? *Proteins* **57,** 433–43 (2004).

7. Warner, H. R., Duncan, B. K., Garrett, C. & Neuhard, J. Synthesis and metabolism of uracil-containing deoxyribonucleic acid in Escherichia coli. *J. Bacteriol.* **145,** 687–95 (1981).

8. Studebaker, a W., Lafuse, W. P., Kloesel, R. & Williams, M. V. Modulation of human dUTPase using small interfering RNA. *Biochem. Biophys. Res. Commun.* **327,** 306–10 (2005).

9. Merényi, G. *et al.* Cellular response to efficient dUTPase RNAi silencing in stable HeLa cell lines perturbs expression levels of genes involved in thymidylate metabolism. *Nucleosides. Nucleotides Nucleic Acids* **30,** 369–90 (2011).

10. Hirmondó, R., Lopata, A., Vértessy, B. G. & Tóth, J. Distinct control of dNTP biosynthesis and genome integrity maintenance by dUTPases. *Submitt. Manuscr.*

11. Castillo-Acosta, V. M., Estévez, A. M., Vidal, A. E., Ruiz-Perez, L. M. & González-Pacanowska, D. Depletion of dimeric all-alpha dUTPase induces DNA strand breaks and impairs cell cycle progression in Trypanosoma brucei. *Int. J. Biochem. Cell Biol.* **40,** 2901–13 (2008).

12. Castillo-Acosta, V. M. *et al.* Increased uracil insertion in DNA is cytotoxic and increases the frequency of mutation, double strand break formation and VSG switching in Trypanosoma brucei. *DNA Repair (Amst).* **11,** 986–95 (2012).

13. Békési, A. *et al.* Developmental regulation of dUTPase in Drosophila melanogaster. *J. Biol. Chem.* **279,** 22362–70 (2004).

14. Johansson, E., Bjornberg, O., Nyman, P. O. & Larsen, S. Structure of the bifunctional dCTP deaminase-dUTPase from Methanocaldococcus jannaschii and its relation to other homotrimeric dUTPases. *J. Biol. Chem.* **278,** 27916–22 (2003).

15. Johansson, E. *et al.* Structures of dCTP deaminase from Escherichia coli with bound substrate and product: reaction mechanism and determinants of mono- and bifunctionality for a family of enzymes. *J. Biol. Chem.* **280,** 3051–9 (2005).

16. Helt, S. S. *et al.* Mechanism of dTTP inhibition of the bifunctional dCTP deaminase:dUTPase encoded by Mycobacterium tuberculosis. *J. Mol. Biol.* **376,** 554–69 (2008).

17. Vértessy, B. G. & Tóth, J. Keeping uracil out of DNA: physiological role, structure and catalytic mechanism of dUTPases. *Acc. Chem. Res.* **42,** 97–106 (2009).

18. Price, a R. Bacteriophage PBS2-induced deoxycytidine triphosphate deaminase in Bacillus subtilis. *J. Virol.* **14,** 1314–7 (1974).

19. Björnberg, O., Neuhard, J. & Nyman, P. O. A bifunctional dCTP deaminase-dUTP nucleotidohydrolase from the hyperthermophilic archaeon Methanocaldococcus jannaschii. *J. Biol. Chem.* **278,** 20667–72 (2003).

20. Johansson, E. *et al.* Regulation of dCTP deaminase from Escherichia coli by nonallosteric dTTP binding to an inactive form of the enzyme. *FEBS J.* **274,** 4188–98 (2007).

21. Mol, C. D., Harris, J. M., McIntosh, E. M. & Tainer, J. a. Human dUTP pyrophosphatase: uracil recognition by a beta hairpin and active sites formed by three separate subunits. *Structure* **4,** 1077–92 (1996).

22. Fiser, a & Vértessy, B. G. Altered subunit communication in subfamilies of trimeric dUTPases. *Biochem. Biophys. Res. Commun.* **279,** 534–42 (2000).

23. Dubrovay, Z. *et al.* Multidimensional NMR identifies the conformational shift essential for catalytic competence in the 60-kDa Drosophila melanogaster dUTPase trimer. *J. Biol. Chem.* **279,** 17945–50 (2004).

24. Nord, J., Kiefer, M., Adolph, H. W., Zeppezauer, M. M. & Nyman, P. O. Transient kinetics of ligand binding and role of the C-terminus in the dUTPase from equine infectious anemia virus. *FEBS Lett.* **472,** 312–6 (2000).

25. Tóth, J., Varga, B., Kovács, M., Málnási-Csizmadia, A. & Vértessy, B. G. Kinetic mechanism of human dUTPase, an essential nucleotide pyrophosphatase enzyme. *J. Biol. Chem.* **282,** 33572–82 (2007).

26. Larsson, G., Nyman, P. O. & Kvassman, J. O. Kinetic characterization of dUTPase from Escherichia coli. *J. Biol. Chem.* **271,** 24010–6 (1996).

27. Quesada-Soriano, I. *et al.* Kinetic properties and specificity of trimeric Plasmodium falciparum and human dUTPases. *Biochimie* **92,** 178–86 (2010).

28. Thymark, M., Johansson, E., Larsen, S. & Willemoës, M. Mutational analysis of the nucleotide binding site of Escherichia coli dCTP deaminase. *Arch. Biochem. Biophys.* **470,** 20–6 (2008).

29. Nord, J., Larsson, G., Kvassman, J. O., Rosengren, a M. & Nyman, P. O. dUTPase from the retrovirus equine infectious anemia virus: specificity, turnover and inhibition. *FEBS Lett.* **414,** 271–4 (1997).

30. Laine, E., Auclair, C. & Tchertanov, L. Allosteric communication across the native and mutated KIT receptor tyrosine kinase. *PLoS Comput. Biol.* **8,** e1002661 (2012).

31. Pécsi, I. *et al.* Nucleotide pyrophosphatase employs a P-loop-like motif to enhance catalytic power and NDP/NTP discrimination. *Proc. Natl. Acad. Sci. U. S. A.* **108,** 14437–42 (2011).

32. Martin, A., Baker, T. A. & Sauer, R. T. Rebuilt AAA + motors reveal operating principles for ATP-fuelled machines. *Nature* **437,** 1115–20 (2005).

33. Varga, B. *et al.* Active site closure facilitates juxtaposition of reactant atoms for initiation of catalysis by human dUTPase. *FEBS Lett.* **581,** 4783–8 (2007).

34. Pecsi, I., Leveles, I., Harmat, V., Vertessy, B. G. & Toth, J. Aromatic stacking between nucleobase and enzyme promotes phosphate ester hydrolysis in dUTPase. *Nucleic Acids Res.* **38,** 7179–86 (2010).

35. Barabás, O., Pongrácz, V., Kovári, J., Wilmanns, M. & Vértessy, B. G. Structural insights into the catalytic mechanism of phosphate ester hydrolysis by dUTPase. *J. Biol. Chem.* **279,** 42907–15 (2004).

36. Lopata, A. *et al.* Mutations Decouple Proton Transfer from Phosphate Cleavage in the dUTPase Catalytic Reaction. *ACS Catal.* **5,** 3225–3237 (2015).

37. Miyahara, S. *et al.* Discovery of highly potent human deoxyuridine triphosphatase inhibitors based on the conformation restriction strategy. *J. Med. Chem.* **55,** 5483–96 (2012).

38. Takács, E., Grolmusz, V. K. & Vértessy, B. G. A tradeoff between protein stability and conformational mobility in homotrimeric dUTPases. *FEBS Lett.* **566,** 48–54 (2004).

39. Kovári, J. *et al.* Altered active site flexibility and a structural metal-binding site in eukaryotic dUTPase: kinetic characterization, folding, and crystallographic studies of the homotrimeric Drosophila enzyme. *J. Biol. Chem.* **279,** 17932–44 (2004).

40. Hofer, A., Crona, M., Logan, D. T. & Sjöberg, B.-M. DNA building blocks: keeping control of manufacture. *Crit. Rev. Biochem. Mol. Biol.* **47,** 50–63 (2012).

41. Mathews, C. K. Deoxyribonucleotides as genetic and metabolic regulators. *FASEB J.* 1–9 (2014). doi:10.1096/fj.14-251249

42. Marx, A. & Alian, A. The First Crystal Structure of a dTTP-bound Deoxycytidylate Deaminase Validates and Details the Allosteric-Inhibitor Binding Site. *J. Biol. Chem.* **290,** 682–90 (2015).

43. Ellims, P. H., Kao, A. Y. & Chabner, B. A. Kinetic behaviour and allosteric regulation of human deoxycytidylate deaminase derived from leukemic cells. *Mol. Cell. Biochem.* **57,** 185–190 (1983).

44. Mollgaard, H. & Neuhard, J. Deoxycytidylate deaminase from bacillus subtilis. Purification, characterization, and physiological function. *J. Biol. Chem.* **253,** 3536–3542 (1978).

45. Sánchez, A. *et al.* Replication Fork Collapse and Genome Instability in dCMP Deaminase Mutant. *Mol. Cell. Biol.* **1,** (2012).

46. Glasner, M. E., Gerlt, J. A. & Babbitt, P. C. Evolution of enzyme superfamilies. *Current Opinion in Chemical Biology* **10,** 492–497 (2006).

47. Gadsden, M. H., McIntosh, E. M., Game, J. C., Wilson, P. J. & Haynes, R. H. dUTP pyrophosphatase is an essential enzyme in Saccharomyces cerevisiae. *EMBO J.* **12,** 4425–31 (1993).

48. Castillo-Acosta, V. M. *et al.* Pyrimidine requirements in deoxyuridine triphosphate nucleotidohydrolase deficient Trypanosoma brucei mutants. *Mol. Biochem. Parasitol.* **187,** 9–13 (2013).

49. Kouzminova, E. A. & Kuzminov, A. Chromosomal fragmentation in dUTPase-deficient mutants of Escherichia coli and its recombinational repair. *Mol. Microbiol.* **51,** 1279–95 (2004).

50. Varga, B. *et al.* Active site of mycobacterial dUTPase: structural characteristics and a built-in sensor. *Biochem. Biophys. Res. Commun.* **373,** 8–13 (2008).

Figure legends

Figure 1 Overview of the dTTP biosynthesis pathways

The three dimensional structures of the nucleotides were extracted from pdb files (dCTP: 1XS4; dUTP: 2V9X; dUMP: 1SNF; dTMP: 1TMK; dTTP: 2QXX; dCMP: 1B5E; dThd: 2V9X) and are shown as atomic colored sticks (C: grey, O: red; N: blue; P: orange). Circled chemical groups call attention to the differences relevant to the enzymatic reactions that transform pyrimidine nucleotides into each other.

Figure 2 Structure and communication in the homotrimers of the dUTPase superfamily

A, "Topview" of the superpositioned core structures of a dUTPase (from *Mycobacterium tuberculosis*, PDB: 2PY4) and a bifunctional DCD-DUT (also from *Mycobacterium tuberculosis*, PDB: 2QLP). The substrate analog dUPNPP (yellow sticks) in complex with Mg^{2+} ions (yellow spheres) is also shown within the dUTPase structure to highlight the active sites. ***B,*** Upper left corner: "side" view of the superpositioned enzyme cores from panel A. The position of the enlarged cross-section plane is indicated by the yellow sticks. Concerted conformational switch within the central channel of DCD-DUT is shown by superposing the apo enzyme in active conformation (PDB: 2QLP) with the dTTP bound enzyme in inactive conformation (PDB: 2QXX). Arrows highlight the most important conformational changes. Note, that only the inactive conformation can accommodate the methyl group of dTTP (grey sticks, Mg^{2+} ions: grey spheres). ***C,*** Schematic representation of active site communication within the dUTPase superfamily. Grey color at the active sites represents enzymatic inactivity. In DCD (-DUT), arrows in the central channel indicate that the inactive conformation is spread through the central channel in a concerted way.

Figure 3 Schematic representation of the covalent trimer concept

A, Schematic representation of the assembly of the $hDUT^{F158W}$ dUTPase. Green spheres represent the sensor-bearing $hDUT^{F158W}$ subunits. The structures reaching out from the subunits represent the swapping C-terminal arm of dUTPase. Yellow stars mark the tryptophan serving as intrinsic fluorescence signal of the enzyme conformations. The pink sphere indicates a Mg^{2+} ion. ***B,*** Schematic representation of the covalent pseudotrimers. The projection of the swapping arms with color transition represents the flexible linkers connecting the C-terminus of one dUTPase protomer to the N-terminus of another one. Different colors of the protomers represent the possible heterogeneity within the trimer, i.e. every protomer can be changed independently from each other.

Figure 4 Asymmetric hybrid enzymes exhibit non-cooperative kinetics in the different reaction steps

A, Schematic representation of the created hybrids (covalent heterotrimers). Blue, red and yellow spheres represent dUTPase protomers containing the D102N, A98F and T148STOP mutations, respectively. Note, that all protomers contain the F158W mutation as well, except for the T148STOP mutant. Grey areas indicate enzymatic inactivity. ***B,*** Steady-state kinetics

of human dUTPase constructs: WWW (solid square), WWN (solid triangles), WNN (open triangles), WWF (solid stars), WWS (solid circle). Smooth lines through the data are hyperbolic fits yielding V_{max}= 7.9 ± 0.5 for WWW, V_{max}= 4.4 ± 0.2 for WWF, V_{max}= 3.8 ± 0.2 for WWN, V_{max}= 1.8 ± 0.1 for WNN, V_{max}= 2.9 ± 0.3 for WWS. K_M values are listed in Table I. ***C,*** Comparison of the catalytic constants (striped bar) and apparent catalytic constants (grey bar) for determined by single turnover (transient kinetics) and steady-state experiments, respectively. See also Table I. for the data. ***D,*** Fluorescence intensity titrations upon dUTP binding to the various dUTPase constructs measured by stopped-flow (the symbol code is identical to that in panel B). Smooth lines through data are hyperbolic fits yielding K_d values summarized in Table I.

Figure 5 Mg^{2+} binding to the central channel reduces the flexibility of the dUTPase trimer

A, Predicted Mg^{2+} binding sites (pink) within the central channel of human dUTPase (PDB: 1Q5H, colored by subunits). The residues constituting the channel wall are shown as surface while the rest of the molecule is shown as cartoon representation. The Tyr residues possibly responsible for the change in the near UV spectra upon Mg^{2+} binding are shown in blue. Active sites are highlighted by the bound dUDP (shown as sticks with atomic coloring). ***B,*** Near UV and Far UV (inset) spectra of $hDUT^{F158W}$ in the presence (dash-dot-dot) and in the absence (solid line) of 5 mM $MgCl_2$. The spectrum of the buffer is marked by dash-dot line. ***C,*** Thermal unfolding of $hDUT^{F158W}$ in the presence and in the absence of 5 mM Mg^{2+}. Smooth lines through the data are Boltzmann fits. The melting temperatures (transition midpoints) are Tm = 59.8 ± 0.2 °C in the presence of $MgCl_2$ and Tm = 58.4 ± 0.2 °C in the absence of $MgCl_2$ (n=3). Errors represents SD. ***D,*** Limited trypsinolysis of $hDUT^{F158W}$ and $mtDUT^{H145W}$ performed in the presence and in the absence of 5 mM $MgCl_2$. The open gray arrow head, the black arrow head and the open black arrow head indicate the intact, the N-terminal cleaved and the N- and C-terminal cleaved enzymes, respectively. The densitometric analysis of the relative amount of the core enzyme (intact enzyme + N-terminal cleaved enzyme + N- and C-terminal cleaved enzyme) is shown in Supplementary Figure 5D.

Figure 6 Stabilization of the central channel hinders conformational coupling with the active sites in dUTPases

A, Sequence comparison of the allosteric loop region within the dUTPase superfamily. The alignment was created by clustalW with minimal manual editing. Allosteric loop, yellow highlight; the uracil binding cleft, underlined; conserved motifs, grey highlight; uracil ring coordination, bold. Amino acid conservation is distinguished by: identity (*****), strong similarity (**:**) and weak similarity (.). ***B,*** Superposition of the 3D structures of representative dUTPase superfamily enzymes from panel A (PDB: *E. coli* DCD – 1XS1, hDUT – 2HQU, EIAV DUT – 1DUC, *E. coli* DUT – 1RN8, MTB DUT – 3HZA). The superposition was performed by the alignment of the bound nucleotides using PyMol. Only the main chain atoms of the proteins and the nucleoside part of the ligands are shown for clarity. The color code refers to the proteins in panel A. Note the structural variance in the allosteric loop. ***C-E,*** Cross section of the central channel of hDUT (1Q5H), *E. coli* DUT and MTB DUT at the level of the uracil binding pocket. The side chains within the central channel and the bound ligands are shown as sticks with atomic coloring. The Mg^{2+} ion is represented as blue non-

bound sphere. In **panel D,** the longitudinal view of the threefold trimer interface (two subunits are shown) of the *E. coli* DUT is also shown using surface representation with atomic coloring to highlight the hydrophobic character of the central channel.

Table 1

	k_{cat} (s^{-1}) [##]	k_{sto} (s^{-1}) [##]	K_M (μM) [#]	$K_{d,dUTP}$ (μM) [#]
hDUT^{F158W}	8 ± 3[*]	6.4[*]	3.6 ± 1.9[*]	0.83[*]
WWW	6.9 ± 0.5	6.33 ± 0.03	1.7 ± 0.5	0.29 ± 0.02
WWF	4.1 ± 0.5	6.13 ± 0.05	0.4 ± 0.3	0.29 ± 0.10
WWN	3.7 ± 0.3	6.31 ± 0.05	0.4 ± 0.3	0.59 ± 0.08
WNN	2.0 ± 0.1	5.72 ± 0.13	2.1 ± 0.5	0.29 ± 0.03
WWS	3.2 ± 0.3	6.26 ± 0.04	2.5 ± 1.2	0.70 ± 0.02

*Data from Toth et al 2007 JBC [25]

[#] Errors represent the fitting error

[##] Errors represent the standard error (SE)

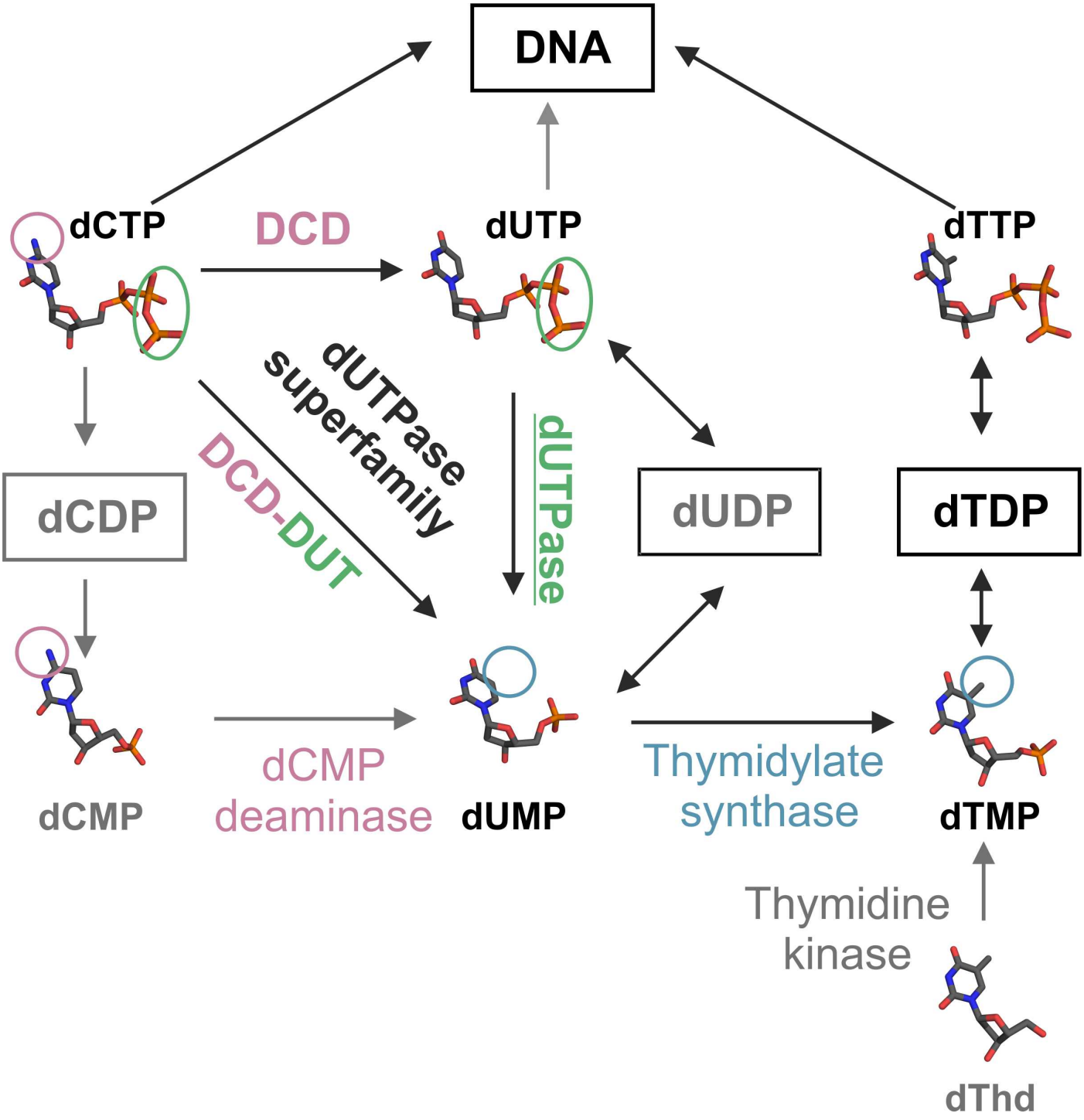
DNA
dCTP
DCD
dUTP
dTTP
dUTPase superfamily
DCD-DUT
dUTPase
dCDP
dUDP
dTDP
dCMP
dCMP deaminase
dUMP
Thymidylate synthase
dTMP
Thymidine kinase
dThd

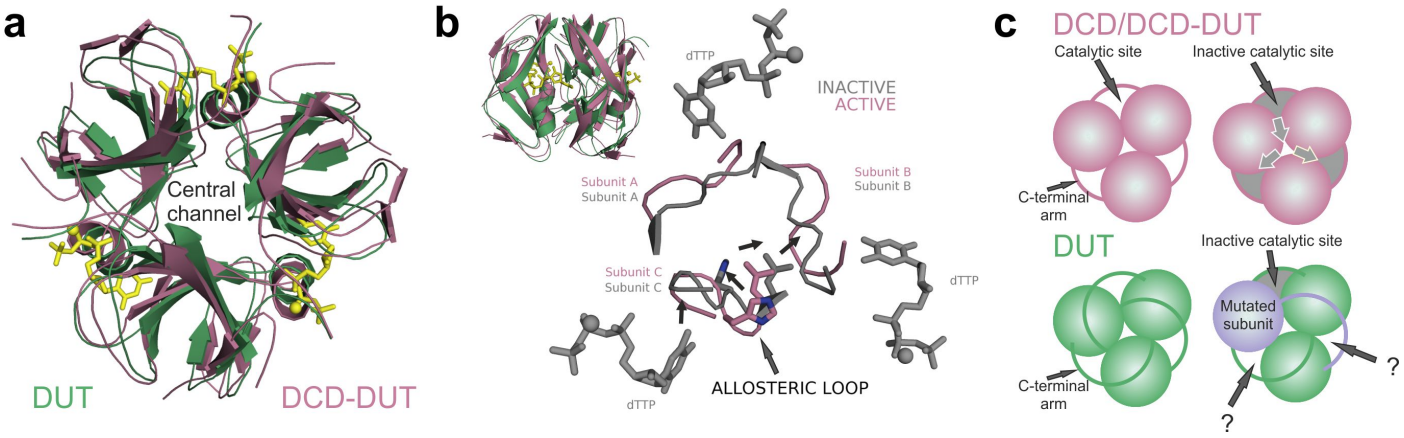
a
Central channel
DUT
DCD-DUT
b
dTTP
INACTIVE
ACTIVE
Subunit A
Subunit A
Subunit B
Subunit B
Subunit C
Subunit C
dTTP
dTTP
ALLOSTERIC LOOP
c
DCD/DCD-DUT
Catalytic site
Inactive catalytic site
C-terminal arm
DUT
Inactive catalytic site
Mutated subunit
C-terminal arm
?
?

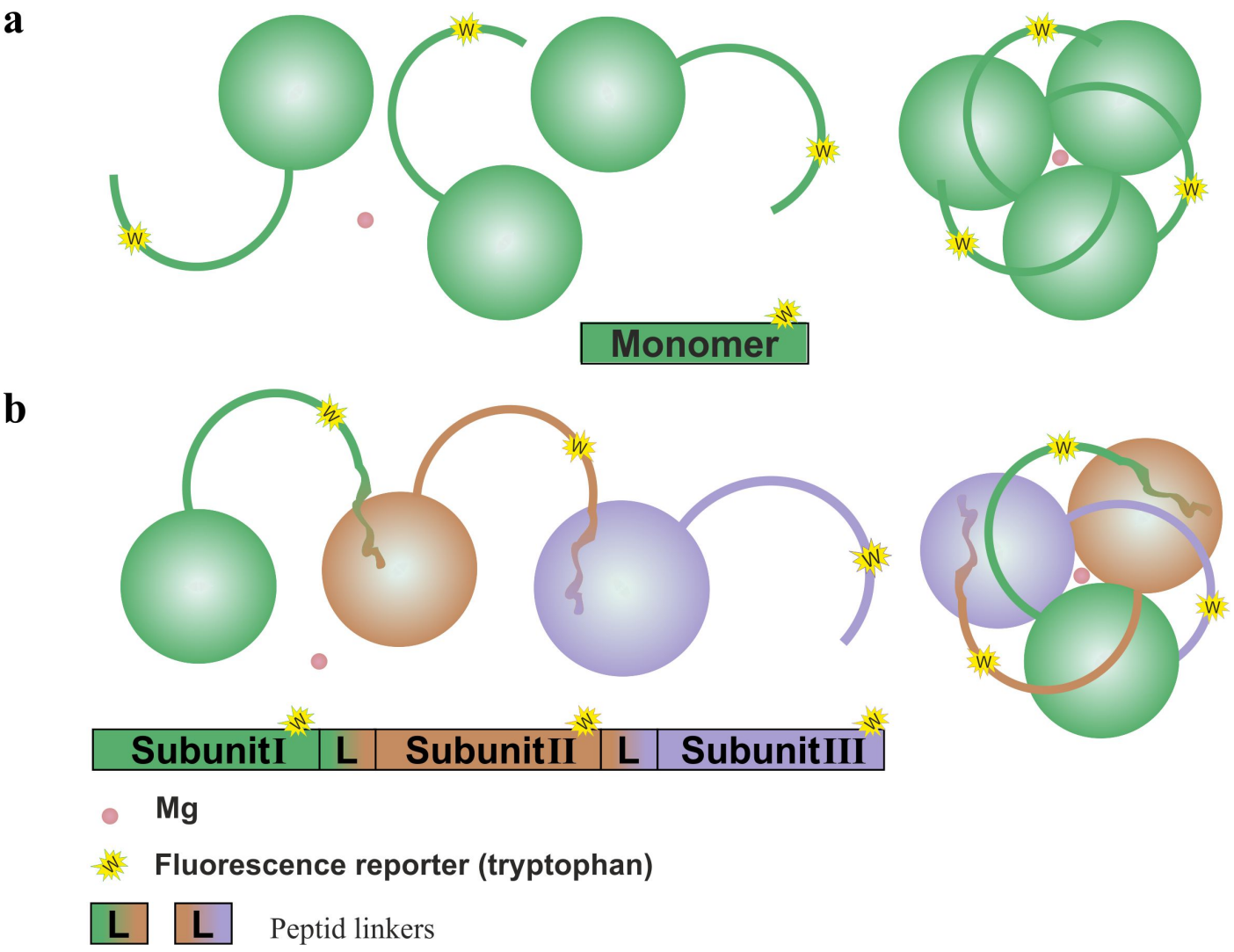
a
W
Monomer
b
SubunitI
L
SubunitII
L
SubunitIII
Mg
Fluorescence reporter (tryptophan)
L
L
Peptid linkers

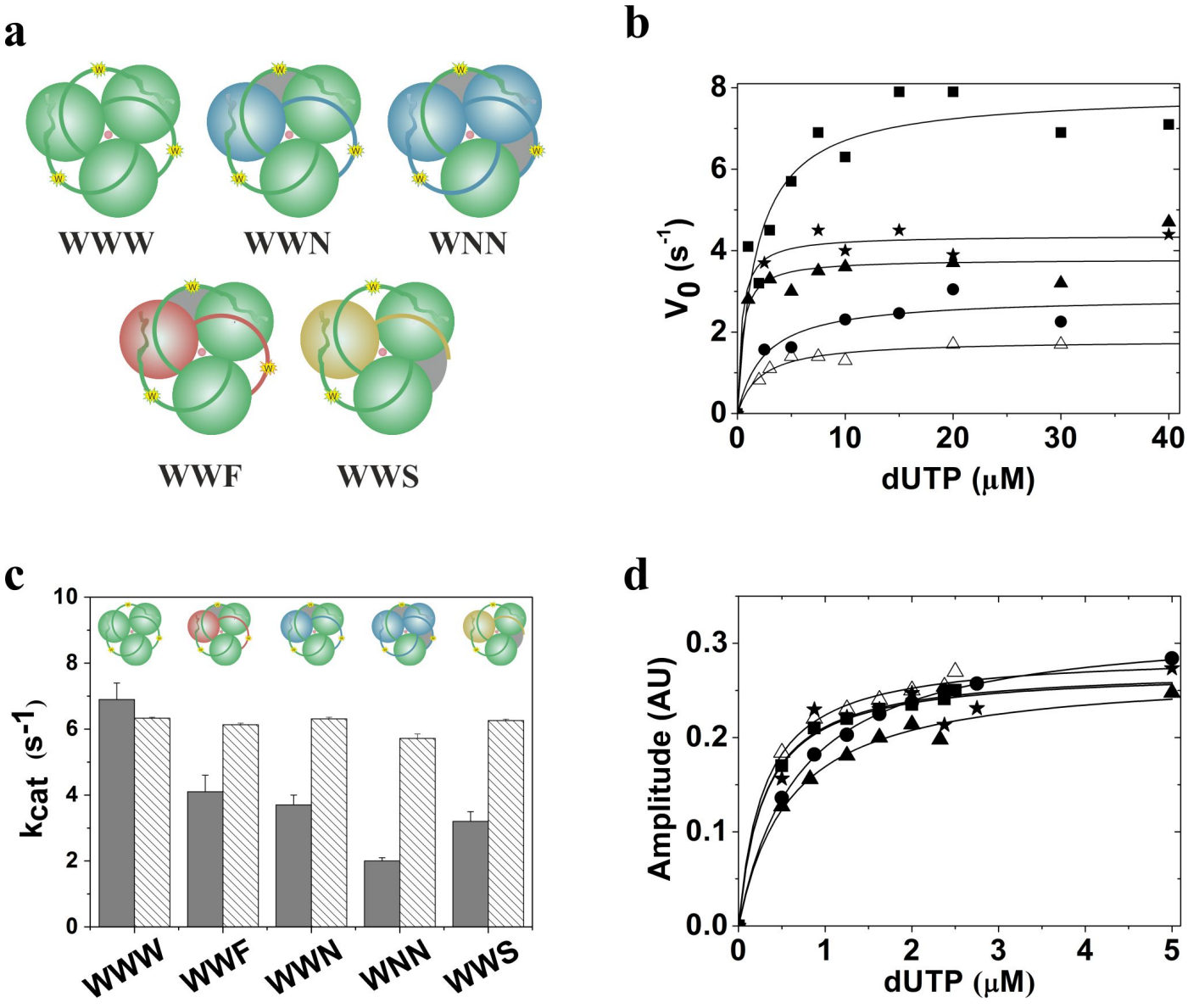
a
WWW
WWN
WNN
WWF
WWS
b
V0 (s-1)
dUTP (μM)
c
kcat (s-1)
WWW
WWF
WWN
WNN
WWS
d
Amplitude (AU)
dUTP (μM)

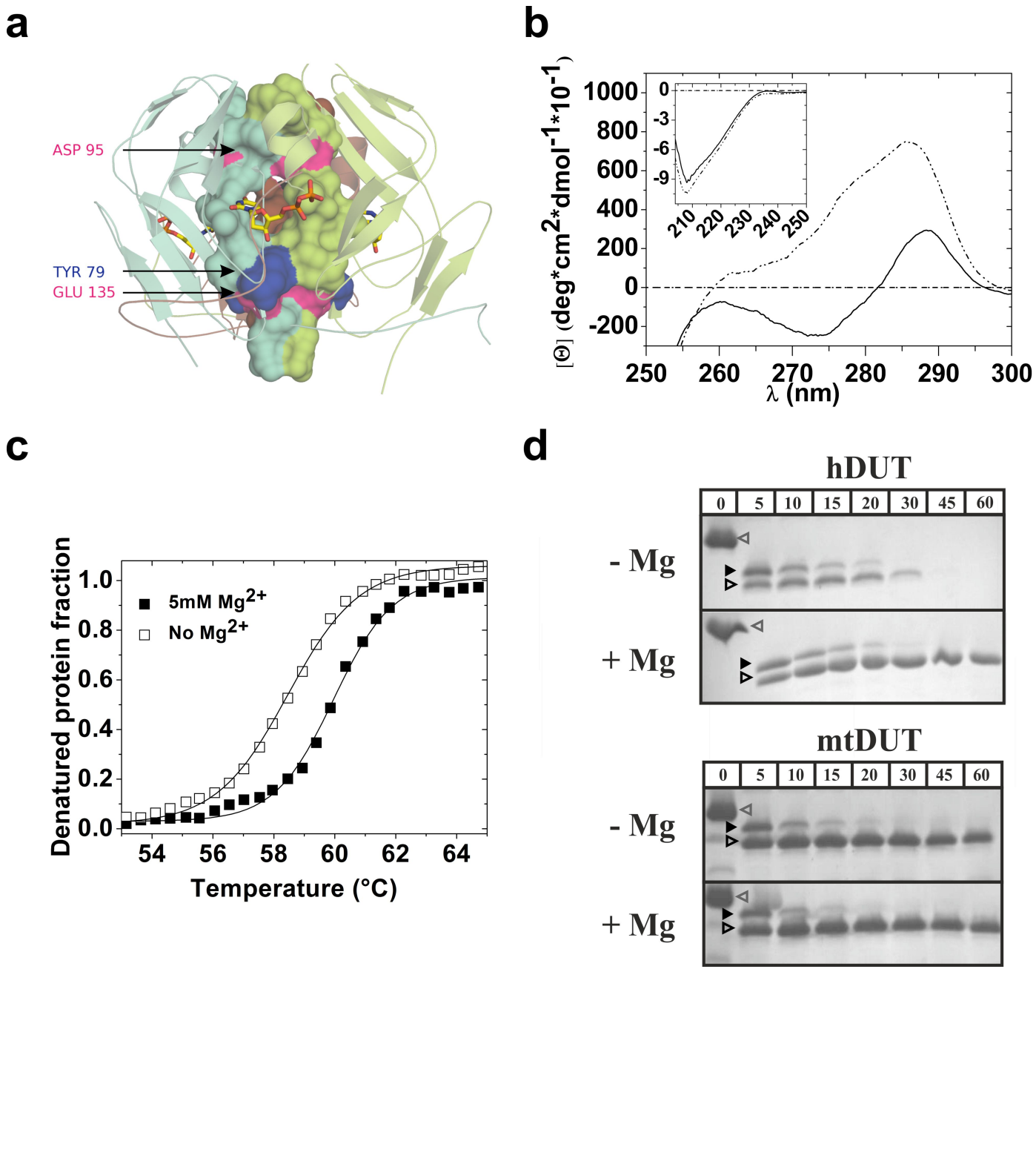
a
ASP 95
TYR 79
GLU 135
b
[Θ] (deg*cm2*dmol-1*10-1)
1000
800
600
400
200
0
-200
250
260
270
280
290
300
λ (nm)
0
-3
-6
-9
210
220
230
240
250
c
Denatured protein fraction
1.0
0.8
0.6
0.4
0.2
0.0
5mM Mg2+
No Mg2+
54
56
58
60
62
64
Temperature (°C)
d
hDUT
0
5
10
15
20
30
45
60
- Mg
+ Mg
mtDUT
0
5
10
15
20
30
45
60
- Mg
+ Mg

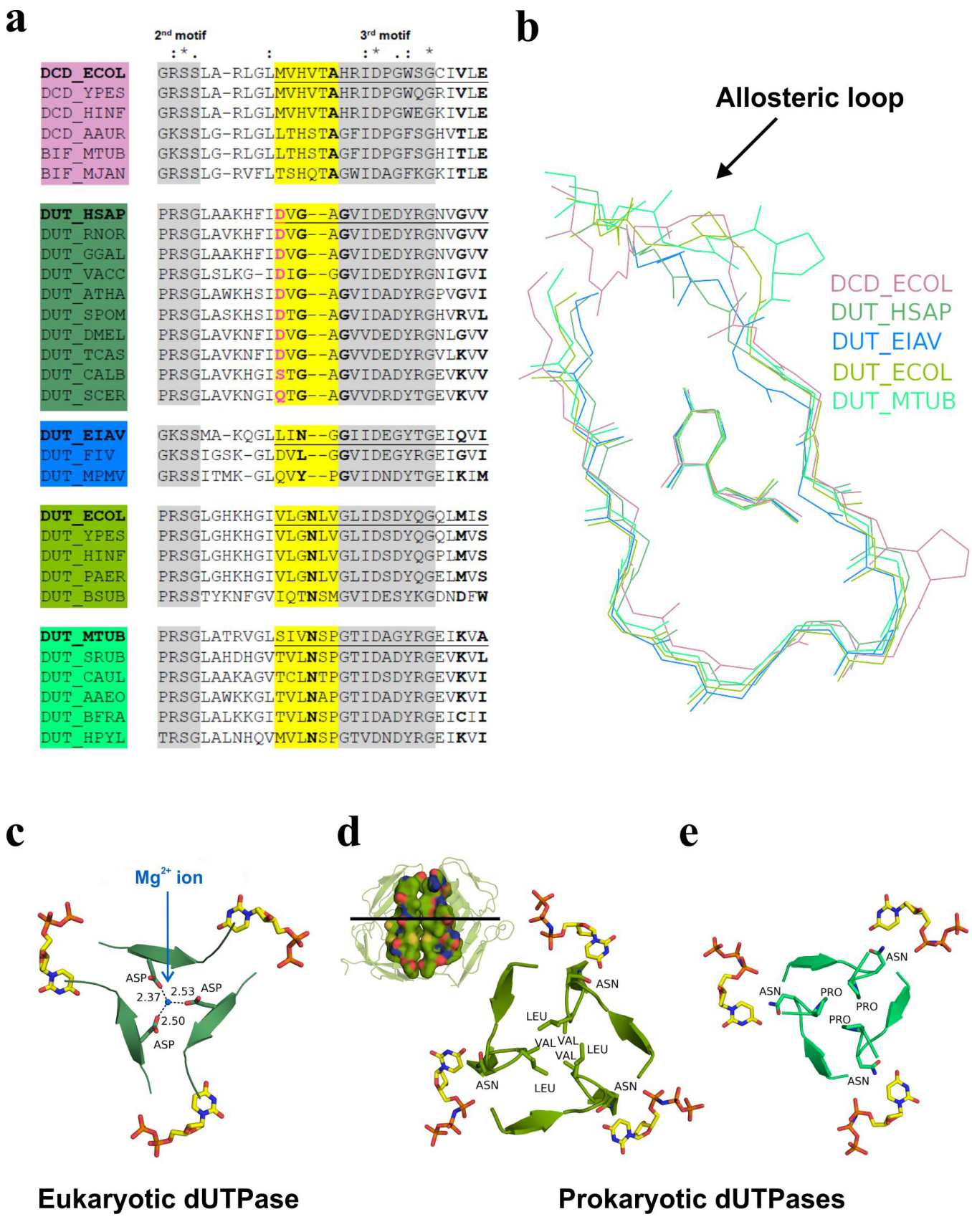
a
2nd motif
3rd motif
DCD_ECOL GRSSLA-RLGLMVHVTAHRIDPGWSGCIVLE
DCD_YPES GRSSLA-RLGLMVHVTAHRIDPGWQGRIVLE
DCD_HINF GRSSLA-RLGLMVHVTAHRIDPGWEGKIVLE
DCD_AAUR GKSSLG-RLGLLTHSTAGFIDPGFSGHVTLE
BIF_MTUB GKSSLG-RLGLLTHSTAGFIDPGFSGHITLE
BIF_MJAN GRSSLG-RVFLTSHQTAGWIDAGFKGKITLE
DUT_HSAP PRSGLAAKHFIDVG--AGVIDEDYRGNVGVV
DUT_RNOR PRSGLAVKHFIDVG--AGVIDEDYRGNVGVV
DUT_GGAL PRSGLAAKHFIDVG--AGVIDEDYRGNVGVV
DUT_VACC PRSGLSLKG-IDIG--GGVIDEDYRGNIGVI
DUT_ATHA PRSGLAWKHSIDVG--AGVIDADYRGPVGVI
DUT_SPOM PRSGLASKHSIDTG--AGVIDADYRGHVRVL
DUT_DMEL PRSGLAVKNFIDVG--AGVVDEDYRGNLGVV
DUT_TCAS PRSGLAVKNFIDVG--AGVVDEDYRGVLKVV
DUT_CALB PRSGLAVKHGISTG--AGVIDADYRGEVKVV
DUT_SCER PRSGLAVKNGIQTG--AGVVDRDYTGEVKVV
DUT_EIAV GKSSMA-KQGLLIN--GGIIDEGYTGEIQVI
DUT_FIV GKSSIGSK-GLDVL--GGVIDEGYRGEIGVI
DUT_MPMV GRSSITMK-GLQVY--PGVIDNDYTGEIKIM
DUT_ECOL PRSGLGHKHGIVLGNLVGLIDSDYQGQLMIS
DUT_YPES PRSGLGHKHGIVLGNLVGLIDSDYQGQLMVS
DUT_HINF PRSGLGHKHGIVLGNLVGLIDSDYQGPLMVS
DUT_PAER PRSGLGHKHGIVLGNLVGLIDSDYQGELMVS
DUT_BSUB PRSSTYKNFGVIQTNSMGVIDESYKGDNDFW
DUT_MTUB PRSGLATRVGLSIVNSPGTIDAGYRGEIKVA
DUT_SRUB PRSGLAHDHGVTVLNSPGTIDADYRGEVKVL
DUT_CAUL PRSGLAAKAGVTCLNTPGTIDSDYRGEVKVI
DUT_AAEO PRSGLAWKKGLTVLNAPGTIDADYRGEVKVI
DUT_BFRA PRSGLALKKGITVLNSPGTIDADYRGEICII
DUT_HPYL TRSGLALNHQVMVLNSPGTVDNDYRGEIKVI
b
Allosteric loop
DCD_ECOL
DUT_HSAP
DUT_EIAV
DUT_ECOL
DUT_MTUB
c
Mg2+ ion
ASP
2.37
2.53
ASP
2.50
ASP
d
ASN
LEU
VAL
VAL
VAL
LEU
ASN
LEU
ASN
e
ASN
ASN
PRO
PRO
PRO
ASN
Eukaryotic dUTPase
Prokaryotic dUTPases

Supplementary Results

The linkers in WWW do not influence the dUTPase enzymatic cycle

The WWW construct showed similar enzymatic properties to those of hDUT^{F158W} under steady state conditions (V_{max} = 6.9 ± 1.2 s^{-1}, K_M = 1.3 ± 0.34 μM, Figure 4, Table 1). To confirm that the covalent linkage of the dUTPase monomers does not alter the enzymatic mechanism, we performed transient kinetic analysis as well. We determined the single turnover catalytic rate constant of the WWW enzyme (k_{STO} = 6.2 ± 0.2 s^{-}) and found it almost identical to the one reported for hDUT^{F158W} (k_{STO} = 6.4 ± 0.2 s^{-1} [1]) (Supplementary Figure 1A, Table 1). The substrate binding properties of WWW also proved to be similar to those of hDUT^{F158W} (Supplementary Figure 1B-C). WWW also binds dUTP in two steps. However, the observed rate constants for the collision complex formation were found to be higher than in the case of hDUT^{F158W} indicating that that dUTP binds somewhat faster to the covalently linked enzyme. The observed rate constant of the second binding phase (proposed to be the isomerization of the enzyme-substrate complex [1]) did not depend on the dUTP concentration in the investigated concentration range (high above the K_M). In this concentration range, the observed rate constants for an isomerization step approximate the sum of the forward and the backward rates of the suspected conformational change. In the kinetic model for the hDUT^{F158W}, the rate constants for the isomerization step are k_{iso}= 21.2 s^{-1} and k_{-iso}= 3.7 s^{-1}[1]. Therefore, the obtained k_{obs2} = 30.4 ± 9.13 $s^{-1}$for dUTP binding to WWW corresponds well to the isomerization observed rate constants of a wild type enzyme. This indicates that this step of the enzyme reaction remains unaltered by the linkage of dUTPase monomers. The concentration dependence of the total fluorescence intensity change of the stopped flow time courses was used to determine the K_d of the enzyme.dUTP complexes (Figure 4D). All these parameters determined for WWW and previously for hDUT^{F158W} can be compared in Table 1.
In summary, the only notable change in the enzymatic mechanism was detected in the kinetics of the collision complex formation with the substrate. We propose that the increase in the rate constant of the first dUTP binding step may be due to the altered flexibility of the swapping arm due to the inserted peptide linker. The swapping arm confers the P-loop-like motif that participates in dUTP binding and hydrolysis [2].

Characterization of the mutations applied to create the asymmetric hybrid enzymes

We designed a mutation to impair dUTP binding to the active site of dUTPase. We introduced an aromatic ring into the tight β hairpin of the uracil binding pocket of the active site by the replacement of Ala98 with the bulky Phe. The Phe was expected to prevent ligand binding by excluding its uracil moiety from its cognate binding site (Supplementary Figure 3B). To characterize the mutation, we first created a homotrimer containing the A98F change in each of the three active sites. As expected, the hDUT$^{F158W,\ A98F}$ homotrimer did not exhibit any dUTPase activity (Supplementary Figure 3A). To exclude that the lack of enzymatic activity resulted from a compromised protein structure, we measured the thermal unfolding properties of the hDUT$^{F158W,\ A98F}$ protein. The thermal unfolding curve of hDUT$^{F158W,\ A98F}$ was cooperative and yielded identical melting temperature (T_m) to that of hDUT^{F158W} (Supplementary Figure 3C-D). As the binding of a cognate ligand to the enzyme stabilizes its structure and thus shifts the T_m of the complex higher, we performed the experiment in the

presence of saturating deoxyuracil nucleotides as well (dUMP and dUTP). While a large increase in T_m was observed in the wild type enzyme-nucleotide complexes, the unfolding curve of the hDUT$^{F158W, A98F}$ protein remained unaffected by the nucleotides (Supplementary Figure 3C-D). To further test the stability and nucleotide binding ability of the hDUT$^{F158W, A98F}$ protein, we performed limited trypsinolysis experiments in the presence and absence of nucleotides as well. It was shown earlier that the flexible N- and C-termini become readily cleaved in the apo enzyme while the substrate analog dUPNPP protects the C-terminus against tryptic cleavage [3]. The resulting protein core remains stable for long time[3]. In case of the apo enzyme, the limited trypsinolysis resulted in similar digestion patterns in both hDUT^{F158W} and hDUT$^{F158W, A98F}$ (Supplementary Figure 3E). The protection effect of dUPNPP was well observable in hDUT^{F158W} but was absent in hDUT$^{F158W, A98F}$ (Supplementary Figure 3E). Both the thermal unfolding and the limited trypsinolysis results confirm that the hDUT$^{F158W, A98F}$ protein is well folded but is not able to bind dUTP or dUMP.

The effect of Mg^{2+} binding to WWW

To reinforce the effect of Mg^{2+} binding to the central channel on the global structure of dUTPase, we repeated the CD and thermal denaturation experiments carried out with hDUT^{F158W} (Figure 5B-C) using the WWW construct as well. The near-UV CD spectrum of WWW (Supplementary Figure 5A) showed some differences in the Phe region (250-270 nm) compared with that of hDUT^{F158W}. The hDUT^{F158W} protein contains a Phe (F48) in the flexible N-terminal part. The presence of the linker in WWW probably changes the conformational properties of the linked N-terminus in the second and third subunits. The N-terminal part of the human dUTPase is involved in nuclear import [4] but not in the catalytic reaction [3,4]. The addition of $MgCl_2$ resulted in the same characteristic spectral changes as in hDUT^{F158W}. The far-UV CD spectrum showed no changes upon the addition of $MgCl_2$, similarly to what was observed in hDUT^{F158W} (Supplementary Figure 5B).

The thermal denaturation of the WWW enzyme could not be described with a two-state equilibrium model indicating that the heat-induced unfolding of the covalent trimer occurs in more steps (Supplementary Figure 5C). The analysis of the thermal unfolding curves of WWW revealed two transition midpoints (Supplementary Figure 5C). One of them was identical with the T_m of hDUT^{F158W} (~ 60 °C). The additional T_m was observed around 45 °C and represented the lower fraction of the amplitude. The thermal unfolding of the hDUT^{F158W} homotrimer occurs in one, highly cooperative step (cf. Figure 5C). The less cooperative thermal unfolding curve and the additional, low temperature T_m may indicate a populated folding intermediate of a less stable conformation of WWW due to the linkers. Upon the addition of $MgCl_2$, the T_m values did not show a pronounced change. However, a shift was observed in the proportion of the two transitions. The fraction of the first transition was 0.29 ± 0.04 in the absence and 0.14 ± 0.04 in the presence of $MgCl_2$, indicating that the intermediate state with low T_m is less populated in the presence of Mg^{2+}.

Altogether, these results reinforce that Mg^{2+} binds to the unliganded dUTPase structure and evokes a stabilization effect.

Supplementary References

1. Tóth, J., Varga, B., Kovács, M., Málnási-Csizmadia, A. & Vértessy, B. G. Kinetic mechanism of human dUTPase, an essential nucleotide pyrophosphatase enzyme. *J. Biol. Chem.* **282,** 33572–82 (2007).

2. Pécsi, I. *et al.* Nucleotide pyrophosphatase employs a P-loop-like motif to enhance catalytic power and NDP/NTP discrimination. *Proc. Natl. Acad. Sci. U. S. A.* **108,** 14437–42 (2011).

3. Varga, B. *et al.* Active site closure facilitates juxtaposition of reactant atoms for initiation of catalysis by human dUTPase. *FEBS Lett.* **581,** 4783–8 (2007).

4. Bozóky, Z. *et al.* Calpain-catalyzed proteolysis of human dutpase specifically removes the nuclear localization signal peptide. *PLoS One* **6,** e19546 (2011).

5. Kovári, J. *et al.* Altered active site flexibility and a structural metal-binding site in eukaryotic dUTPase: kinetic characterization, folding, and crystallographic studies of the homotrimeric Drosophila enzyme. *J. Biol. Chem.* **279,** 17932–44 (2004).

6. Barabás, O., Pongrácz, V., Kovári, J., Wilmanns, M. & Vértessy, B. G. Structural insights into the catalytic mechanism of phosphate ester hydrolysis by dUTPase. *J. Biol. Chem.* **279,** 42907–15 (2004).

Supplementary Table 1

Name	For/Rev	R. site	Sequence	Goal
D102N	for	-	GGAGCTGGTGTCATAAATGAAGATTATAGAGGAAATGTTGG	Mutagenesis
	rev	-	CCAACATTTCCTCTATAATCTTCATTTATGACACCAGCTCC	
A98F	for	-	GATGTAGGATTTGGTGTCATAGATG	Mutagenesis
	rev	-	CATCTATGACACCAAATCCTACATC	
Subunit I.	for	Kpn1	GGGGTACCATGCCCTGCTCTGAAGAG	Assembly of WWW with linkers
	rev	BamH1	CGGGATCCGGTCGCGCCGCTGGTGCCGCCTTCGCTGCCGCCGC CTTCGCTGCCGCCCGCGCCGCTCGCATTCTTTCCAGTGGAACC	
Subunit II.	for	BamH1	CGGGATCCATGCCCTGCTCTGAAGAG	
	rev	Pst1	AACTGCAGGGTCGCGCCGCTGGTGCCGCCTTCGCTGCCGCCGC CTTCGCTGCCGCCCGCGCCGCTCGCATTCTTTCCAGTGGAACC	
Subunit III.	for	Pst1	AACTGCAGATGCCCTGCTCTGAAGAG	
	rev	Hind3	CCCAAGCTTTTAATTCTTTCCAGTGGAACC	
Subunit III. change	for	Pst1	CTACGCGGCTGCAGATGCCCTGCTCTGAAGAGACAC	Subunit III. exchange
	rev	Xho1	GCGCCAGCTCGAGTTAATTCTTTCCAGTGGAACC	
Linker1:			ASGAGGSEGGGSEGGTSGATGS	
Linker2:			ASGAGGSEGGGSEGGTSGATLQ	

Supplementary Figures

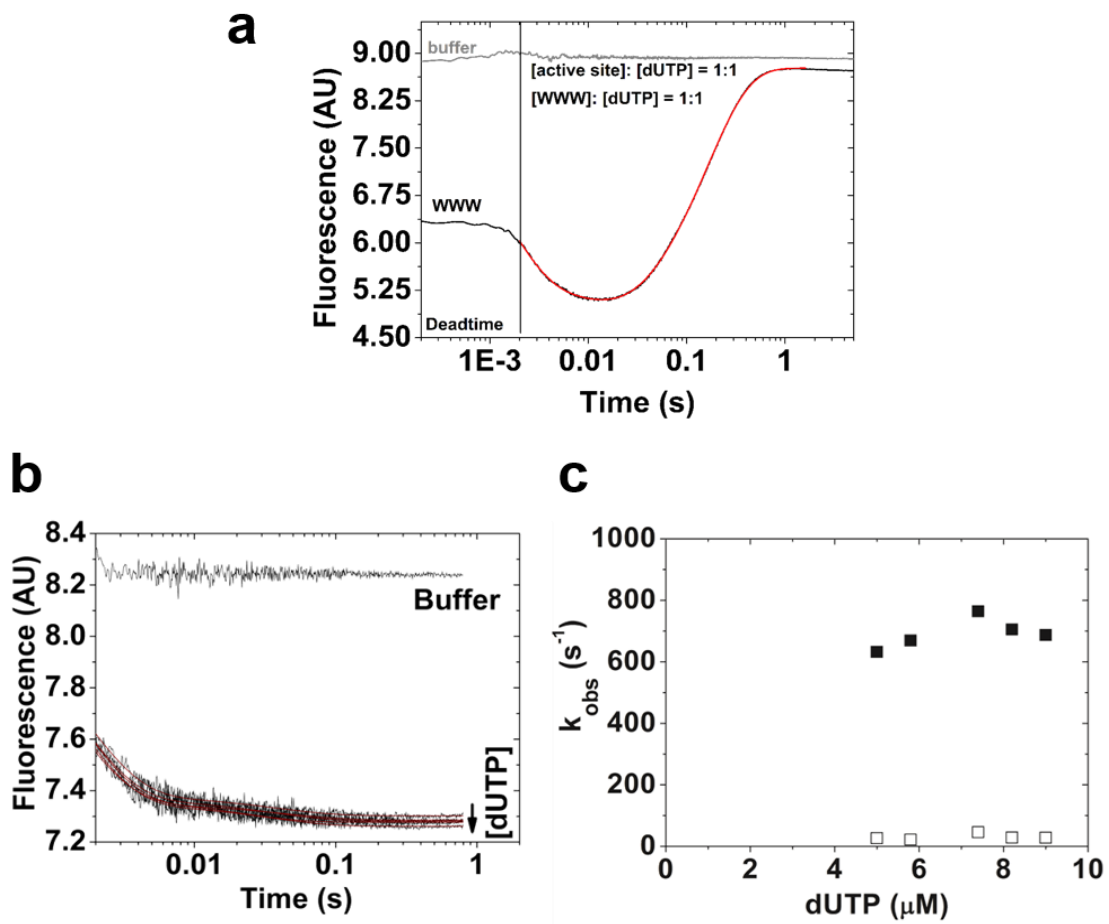

Supplementary Figure 1
Transient kinetic analysis of dUTP binding and hydrolysis by the WWW enzyme

A, Fluorescence time courses recorded upon mixing 20 μM WWW with substoichiometric dUTP or with buffer. The single turnover trace was fitted with triple exponential function (red curve) that yielded 6.24 s^{-1} for the single turnover rate constant (k_{STO}). Both the value of the k_{STO} and the characteristic fluorescence changes of the time course denote wild type enzymatic behavior[1]. ***B,*** Fluorescence time courses recorded upon mixing various concentrations of dUTP with 0.5 μM WWW (postmixing concentration). Smooth lines are double exponential fits to the curves. A large fraction of the amplitude is lost in the dead time of the stopped flow instrument. ***C***, Analysis of the rate constants of the dUTP binding time courses in panel B. The solid squares denote $k_{obs,1}$ for the fast phase of the fitted double exponential. Since a large portion of the amplitude is missing, the concentration dependence of $k_{obs,1}$ did not yield exact association and dissociation constants. Open squares denote $k_{obs,2}$ of the second phase. $k_{obs,2}$ is independent of the dUTP concentration and its mean value is 30.4 ± 9.13 s^{-1}. Based on these results, the WWW enzyme is indistinguishable from the $hDUT^{F158W}$ wild type enzyme[1].

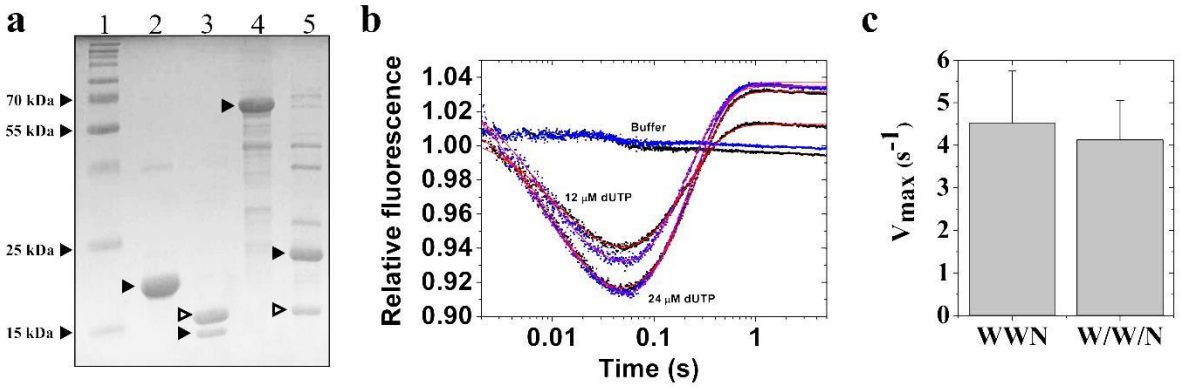

Supplementary Figure 2
Covalent coupling of the dUTPase monomers does not disturb the enzymatic properties of the functional trimers

A, PAGE analysis of the products of limited trypsinolysis. Lane 1: marker; lane 2: hDUT; Lane 3: hDUT treated with tryspin (empty arrow head: N-terminal cleaved protein fragment, black arrowhead: N- and C-terminal cleaved protein fragment); Lane 4: WWN covalent heterotrimer; Lane 5: WWN heterotrimer treated with tryspin. dUPNPP was present to give protection against the cleavage of the C-terminus (contains the catalytically important conserved motif V). The black arrowhead and the empty arrowhead points to monomers with linkers (2 monomers / trimer) and without linker (one monomer / trimer), respectively. Note that an N- and C-terminally cleaved fragment is not present thanks to the protective effect of the bound dUPNPP. ***B,*** Single turnover analysis of intact (WWN) and cleaved (W/W/N) heterotrimers measured by stopped flow. k_{STO} values derived from triple exponential fits (red curves) to the time courses were $5.5 \pm 0.1\ s^{-1}$ (12 μM dUTP) and $5.9 \pm 0.1\ s^{-1}$ (24 μM dUTP) for WWN; $5.6 \pm 0.1\ s^{-1}$ (12 μM dUTP) and $5.3 \pm 0.1\ s^{-1}$ (24 μM dUTP) for W/W/N. Errors represent fitting errors. ***C,*** Steady state activity of the WWN ($4.5 \pm 1.2\ s^{-1}$, n = 3) and of the W/W/N ($4.1 \pm 0.9\ s^{-1}$, n = 2) enzymes.

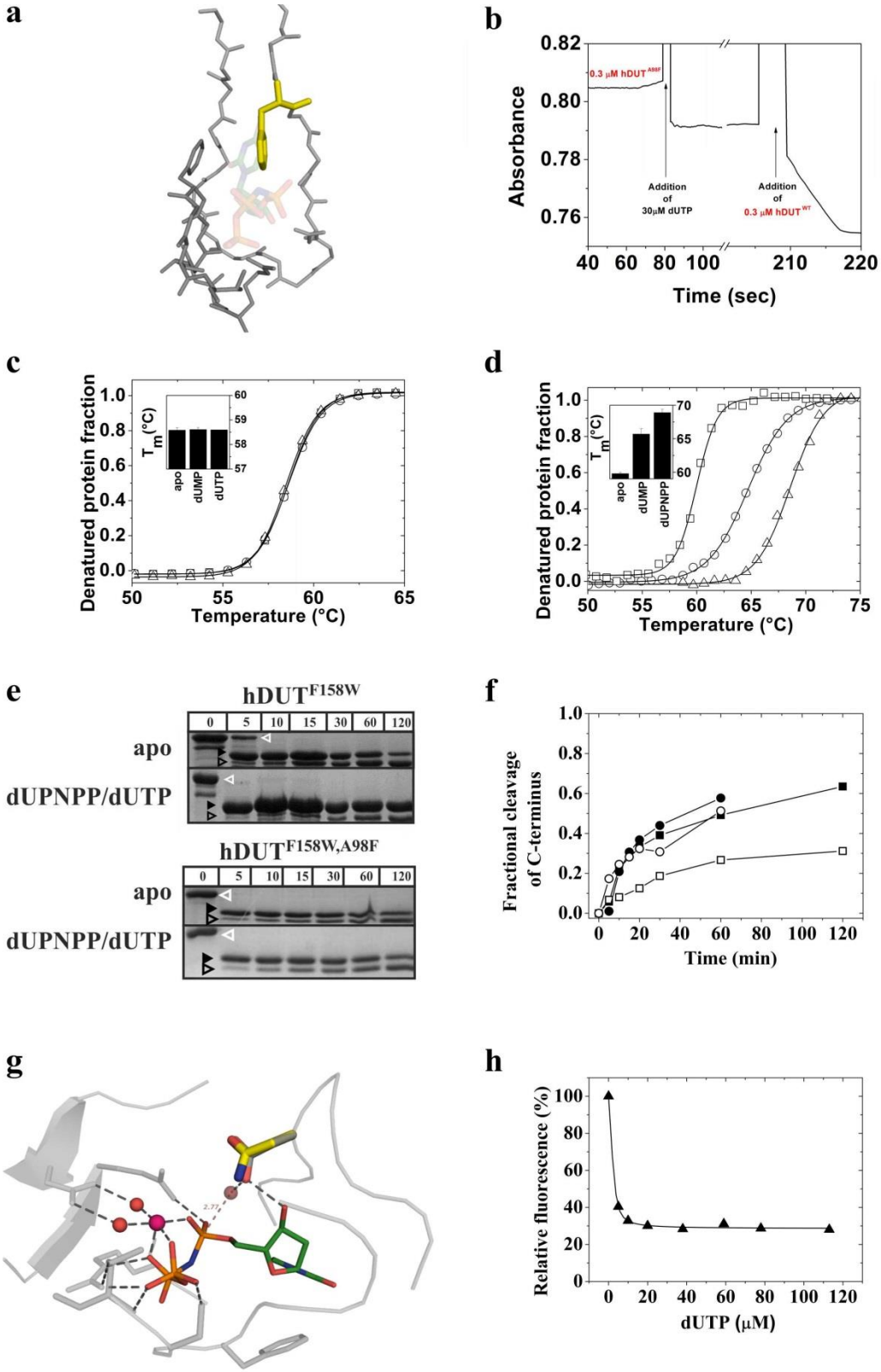

Supplementary Figure 3
Characterization of the A98F and the D102 mutations

A, Structural model of the active site of the A98F mutant hDUT (PyMol). The uracil-binding ß hairpin and the 5th motif from the swapping arm of human dUTPase are shown as grey stick backbone. dUTP is shown as transparent sticks with atomic coloring. The single allowed

conformation of Phe98 in this structure is highlighted by yellow coloring. This structural representation shows that the aromatic ring of Phe98 occupies the binding site of the uracil moiety of the substrate. ***B***, Enzyme activity assay. The A98F protein is premixed in the assay buffer, the dUTPase reaction is initiated by the addition of dUTP. No enzyme activity is detected until the addition of the wild type enzyme that hydrolyzes the intact dUTP. ***C-D***, Thermal unfolding of the A98F mutant (***C***) and of the wild type dUTPase (***D***), respectively, in the absence of nucleotides (square), in the presence of 5 mM dUMP (circle) or 1 mM dUTP (triangle). Smooth lines through the data are Boltzmann fits yielding the melting temperatures presented as bar graph in the inset. ***E***, Limited trypsinolysis of the wild type (hDUT^{F158W}) and the A98F mutant (hDUTF$^{158W,\ A98F}$) in the absence and in the presence of 1 mM dUPNPP. Numbers denote the duration of the tryptic treatment in minutes. The open white arrow head, the solid black arrow head and the open black arrow head shows the intact, the N-terminally cleaved and the N- and C-terminally cleaved enzyme, respectively. ***F,*** Densitometric analysis of the limited trypsinolysis experiment. The graph shows the relative amount of the N- and C-terminally cleaved protein compared to the total amount of protein. It has previously been established that trypsin readily cleaves the flexible N-terminus of dUTPases in a nucleotide-independent manner, while the binding of dUTP or dUPNPP to the enzyme protects the also flexible C-terminus from tryptic digestion[5]. We observe this protection in the wild type enzyme but not in the A98F mutant (see apo vs. dUPNPP/dUTP samples on the gel at 120 min). These data together demonstrate that the A98F substitution hinders the binding of dUTP to the active site while it does not perturb the overall structure (folding, stability) of the protein. ***G***, Structural representation of the D102N mutation in the active site of hDUT (generated by Pymol). The active site building amino acids are shown as grey cartoon and stick backbone. dUTP and residue 102 are shown as sticks with atomic coloring. The Mg^{2+} ion is shown as a magenta sphere, the water molecules are shown as red spheres. D102 coordinates the nucleophile catalytic water molecule while the mutant D102N is not expected to efficiently coordinate this water molecule [6]. ***H,*** Fluorescence intensity titration is shown upon dUTP binding to hDUT$^{F158W,\ D102N}$. The smooth line through the data is a quadratic fit (Equation 1) yielding K_d = 0.7 μM. The quasi wild type relative fluorescence change and K_d (cf. data from the literature [1]) indicate that the substrate binding properties of the hDUT$^{F158W,\ D102N}$ mutant remained unaffected by the D102N mutation.

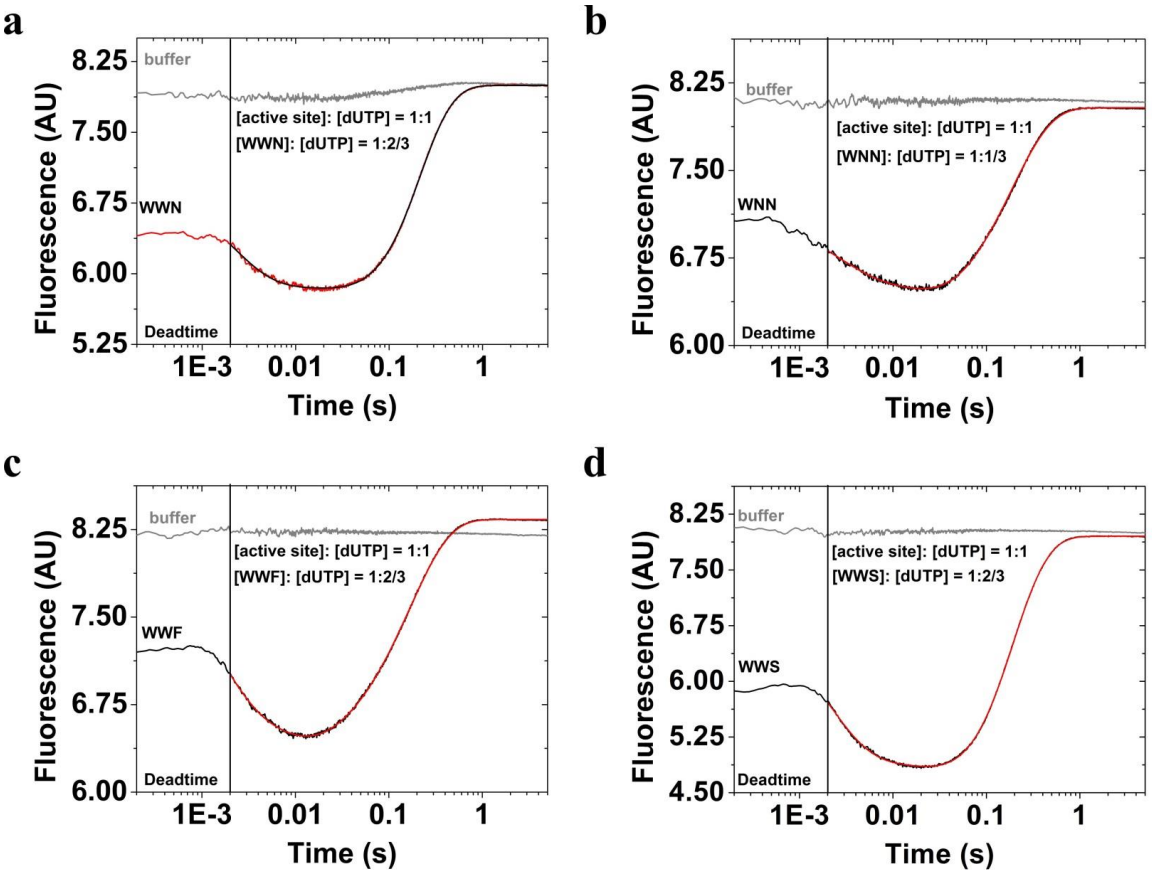

Supplementary Figure 4
Single turnover dUTP hydrolysis time courses of the hybrid enzymes

Fluorescence time courses were recorded upon mixing substoichiometric dUTP with 20μM WWN (***A***), WNN (***B***), WWF (***C***) or WWS (***D***). Single turnover traces were fitted with triple exponential function yielding the following k_{STO} values: 6.43 s^{-1} for WWN, 5.4 s^{-1} for WNN, 5.99 s^{-1} for WWF and 6.26 s^{-1} for WWS. Each measurement was repeated several times, the mean values and errors are shown in Figure 4C and in Table 1. Note that the signal changes are not comparable dues to the optimization of the detector sensitivity in each measurement.

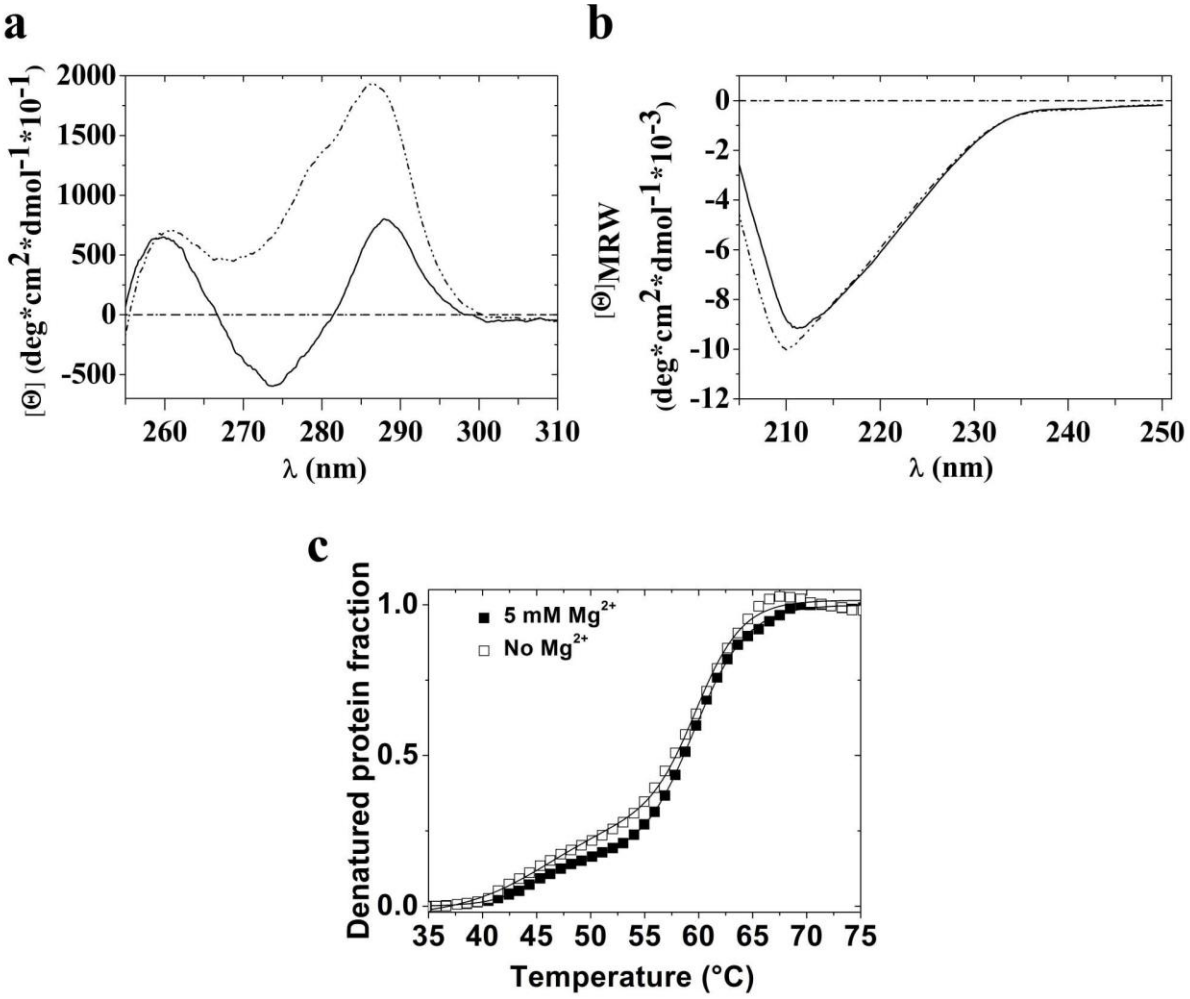

Supplementary Figure 5
The Mg^{2+} binding properties of WWW are similar to those of $hDUT^{F158W}$ (cf. Figure 5)

A, Near UV and ***B,*** far UV CD spectra of WWW in the presence (dash-dot-dot) and in the absence (solid line) of Mg^{2+}. The buffer signal is shown as dash-dash-dot lines. ***C,*** Representative measurements of thermal unfolding of WWW in the presence and in the absence of 5mM Mg^{2+}. Smooth lines through the data are double Boltzman fits. Melting temperatures were determined from the midpoints of transitions and were found to be Tm_1 = 45.1 ± 0.2 °C , Tm_2 = 59.7 ± 0.2 °C in the presence of Mg^{2+} and Tm_1 = 46.6 ± 0.7 °C , Tm_2 = 59.8 ± 0.2 °C in the absence of Mg^{2+} . The fraction of the first transitions was 0.14 ± 0.04 and 0.29 ± 0.04 in the presence and in the absence of Mg^{2+}, respectively. Errors represent SD at n=3.

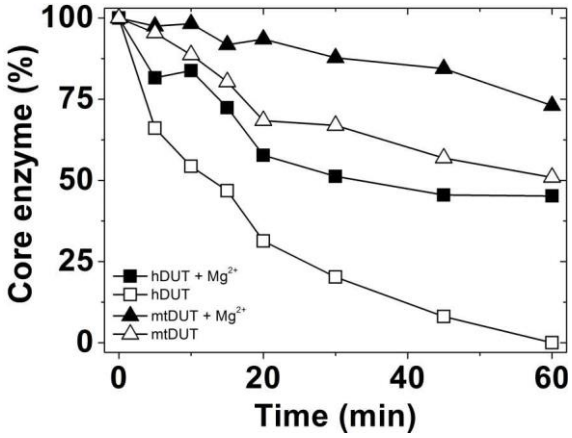

Supplementary Figure 6

Densitometric analysis of the limited trypsinolysis experiment shown in Figure 5D

The relative amount of core enzyme is plotted against time. Core enzyme = intact enzyme + N-terminal cleaved enzyme + N- and C-terminal cleaved enzyme